Sustainable Materials and Technologies 28 (2021) e00253

Contents lists available at ScienceDirect

Sustainable Materials and Technologies

journal homepage: www.elsevier.com/locate/susmat

Environmental performance of miscanthus-lime lightweight concrete using life cycle assessment: Application in external wall assemblies

Fabrice Ntimugura [a,*], Raffaele Vinai [a], Anna B. Harper [a], Pete Walker [b]

[a] College of Engineering, Mathematics and Physical Sciences, University of Exeter, Exeter EX4 4QF, UK
[b] BRE Centre for Innovative Construction Materials, Department of Architecture and Civil Engineering, University of Bath, Bath BA2 7AY, UK

ARTICLE INFO

Article history:
Received 26 November 2020
Received in revised form 20 January 2021
Accepted 25 January 2021

Keywords:
Bio-based building materials
Environmental impact
Thermal insulation
Carbon capture
Miscanthus

ABSTRACT

In the UK context, miscanthus is a potential alternative perennial crop for the development of bio-based building materials. This paper presents the environmental benefits of using miscanthus shives in lightweight blocks and their potential application in wall assemblies. A systemic life cycle assessment (LCA) is carried out for miscanthus-lime blocks, and the effects of binder type and binder content are discussed. The environmental performance-based analysis reveals that miscanthus blocks can capture 135 kg CO_2eq/m^3 for an assumed 100-years life period. The impact analysis using the University of Leiden, institute of environmental science (CML) baseline (v4.4) method shows that 75% of the greenhouse gas emissions are attributable to the production of mineral binders. A reduction of binder to aggregate ratio from 2.0 to 1.5 reduces greenhouse gas emissions by 32.9%. The use of 10 wt% mineral additions can potentially stabilise blocks while having little effect on their overall environmental impacts. The environmental profiles of wall systems incorporating miscanthus-lime blocks have been evaluated in this this study. Combining miscanthus blocks with fired clay bricks enables a potential low carbon retrofitting technique for the current stock of residential buildings in the UK. Timber-framed system filled with miscanthus blocks enables a carbon storage of ~97.3 kg CO_2eq/m^2, which presents a potential carbon offsetting strategy in new-build dwellings. Consideration should be given to the potential negative impacts related to agricultural activities for the production of miscanthus shives. The largest negative environmental impact was ozone layer depletion, where a relative difference of 12.8% was recorded between miscanthus timber-framed wall and a typical solid wall insulated with mineral wool. It appears that miscanthus-lime composites can substantially improve the environmental profile of wall assemblies and sustainability be applied in existing uninsulated masonry walls or incorporated in timber- framed new-build houses.

1. Introduction

Buildings consume large quantities of energy, and it is generally accepted that reducing the energy consumption of buildings is an essential step in lowering the global energy consumption and associated greenhouse gas emissions. In the UK, considerable energy use and environmental impacts are attributed to space heating in residential buildings [1]. Considering the actual global environmental challenges, the European governments and the UK adopted policies towards a more sustainable built environment by regulating the energy performance of buildings. The latter requires sustainable materials and construction systems to be made available to stakeholders in the construction industry. As result of this growing awareness of sustainability concerns, environmentally friendly building materials with potential applications in residential buildings have emerged, and among the most promising are lightweight bio-based building materials. These composite materials are obtained by the association of a high fraction of vegetal aggregates with a mineral binder [2]. Typical bio-based aggregates are obtained from stems (hemp, flax, sunflower), straws (sorghum, maize and miscanthus) or trunks (woodchips) [3]. Hemp remains the most widely used in building materials and studied in literature as a result of long-term research and availability in continental Europe, mainly in France [4]. The extensive literature on hemp-based building materials was recently reviewed by Sáez-Pérez et al. [5].

Residential buildings constitute more than 3/4 of the energy consumption allotted to the built environment in the UK, for a total of ~30% of national energy consumption. Considering the estimated near-30 million dwellings in England, even the smallest contributions on impacts and consumption of resources would be significant at a national scale [6]. In fact, the 2019 report of the Committee on Climate Change (CCC) records a rather poor performance towards expected reductions of the UK's housing emissions. The installations of energy performance upgrading measures in terms of loft and wall insulations stalled to fall at 5% of the 2012 peak market delivery [7].

* Corresponding author.
E-mail addresses: fn246@exeter.ac.uk (F. Ntimugura), r.vinai@exeter.ac.uk (R. Vinai).

https://doi.org/10.1016/j.susmat.2021.e00253
2214-9937/

In general, conventional wall infilling materials exhibit poor to average heat insulating properties [8]. Lightweight materials, such as glass wool, mineral wool, expanded polystyrene and extruded polystyrene, are required to improve resistance to the passage of heat. A recent cradle to gate life cycle assessment (LCA) of conventional insulation materials reports values of global warming potential (GWP100) in the range of 3.25–7.8 $kgCO_2eq$ for ~0.6–1.0 kg of materials, and a consumption of 73–104 MJ for their production [9]. These materials exhibit high environmental impacts, and their ecological efficiency is being brought into question [10]. Focusing on the insulation of building envelopes, LCA studies revealed that the reduction of the building emissions due to the use of modern insulation materials should be corrected considering their embodied energy, carbon footprint and end-of-life issues. While the winter heating loads for a "low-emissions house" can be reduced by a ratio of 10:1 compared to a standard house in the same conditions, life cycle energy can be reduced by 2.1:1 and life cycle impacts reduced by 2.5:1–1.6:1, depending on the indicator [11]. This compels to reassess the relevance of modern insulation materials, and focus on materials selection based on their local availability, renewability and low-energy processing techniques, provided they exhibit acceptable levels of insulation [12]. Bio-based fibres and particles constitute a particular class of materials with such potentials for applications in buildings [13], in particular due to their inherent honeycomb porous structure [14]. In addition to low-energy processing associated with their manufacturing, their biogenic carbon capture and storage is a desirable trait within the context of sustainable, low-energy and affordable building envelopes [15].

A high number of studies on the thermal performance and sustainability of buildings suggests a design-oriented optimisation and operational energy reduction techniques. While the effectiveness of the latter remains undeniable, the embodied energy associated with these techniques stays relatively high. In a typical UK residential house, the embodied carbon represents 20–26% of the total life cycle carbon, with a potential increase of 1–13% associated with regulatory improvements of the thermal performance [16]. In residential and commercial buildings, the embodied energy was found to contribute to 22% and 26% of the total life cycle energy, respectively [17]. Over the past few decades, the thermal performance of building fabrics improved to meet the ever-stringent building regulation requirements, leading to increasingly low thermal transmittance (U-values) and as a consequence, a decrease of heat losses through the new-build envelopes. Furthermore, considering recent developments in the design of most energy-efficient houses embracing the passive design concepts, the embodied energy can account for up to 50% of the total energy consumption [18].

Gonzalez and Navarro have shown that a careful choice of materials can reduce the global warming potential impact by up to 30% in the context of terraced houses in Spain [19]. In such circumstances, the use of sustainable materials can be a point of focus for action to reduce CO_2 emissions. Within the specific context of restoration and preservation of historic buildings, the actual air-permeable materials, and the need then to prevent impermeable layers in the structure of walls precludes the use of closed-foam and plastic-based insulants [20]. Their lack of hygroscopic properties prevents valuable vapour pressure buffering and hence increases the risks of surface and interstitial condensation. In these particular conditions, vapour permeable bio-based building materials offer an unrivaled solution for the restoration works [21]. The aforementioned statements explain the potential use of low-energy bio-based materials as alternatives to standard commonplace energy-intensive insulating materials.

The use of bio-based materials brings about the most sustainable dwellings with acceptable levels of thermal performance and a relatively high level of indoor air quality and comfort. Pierquet et al. [22] investigated the thermal performance and embodied energy of eleven wall systems used in the US. The authors covered an entire range of construction materials from conventional concrete blocks-based walls, improved non-conventional aerated autoclaved concrete walls and straw bale walls. It was reported that non-renewable materials (concrete, steel, synthetic foams) have the lowest long-term energy performance. An LCA study of UK detached, semi-detached and terraced dwellings conducted using GaBi and a combination of Ecoinvent / GaBi databases and available literature data estimated a GWP of 132 million tonnes (Mt) CO_2 eq. per year, leading to a cumulative estimate of 6.6 billion tonnes over 50 years, at the housing sector level [23].

A recent LCA of bio-based materials for insulation of walls in buildings reports a potential opportunity for CO_2 capture and storage in the UK. Ip and Miller reported a carbon storage of 36.08 $kgCO_2eq./m^2$ of a hemp concrete wall [24]. In a comparable French study, Boutin et al. [25] investigated the environmental performance of hemp concrete using a detailed LCA model and similar carbon capture and storage figures were reported ~35.53 $kgCO_2eq./m^2$. Hemp concretes benefit from the biogenic carbon capture of hemp and carbonation of lime binder on the long term. Arrigoni et al. conducted an assessment of the role of carbonation, the impact of mix proportions of components and transportation in the LCA of hemp concrete blocks [26]. The authors experimentally determined the carbonation of hemp concrete blocks using x-ray powder diffraction (XRD) and integrated the acquired quantitative results in the LCA model. After 240 days of curing, the estimated binder carbonation was only 9–12 g per kg of binder. Nevertheless, a negative net carbon balance ~ -12 $kgCO_2eq./m^2$ of wall was reported. Although these figures remain lower than those reported earlier, no less than they corroborated that hemp blocks could act as carbon sinks, even with a limited contribution of binder carbonation. While the rate of carbonation of lime-based binders inside bio-based composites remains arguable, Arehart et al. proposed a theoretical model for carbon storage and sequestration of hemp concrete [27]. The authors estimated the carbonation of lime-based binder between 18.5% and 38.4% with a minimum CO_2 storage potential of 16 $kgCO_2eq./m^2$ of a hemp concrete wall.

Hemp-based building materials have been successful in France due in part to a high production of hemp fibres and shives. In the context of the UK, the production of hemp shives remains limited, and miscanthus is proposed as an alternative source of bio-aggregates [28]. In fact, the UK Committee on Climate Change suggests expanding energy crops by 23,000 ha/year, including miscanthus, and estimates carbon dioxide cuts of ~11 $MtCO_2$ per year from harvested biomass, spurring further research and innovation around the use of miscanthus fibres and composites in buildings [29]. In addition, the CO_2 mitigation potential associated with miscanthus farming, it was proposed to be considered in the greening measures of the EU Common Agricultural policy regulations 2014–2020 [30]. Ben Fradj et al. detailed the potential of miscanthus in bio-based sectors including the development of building materials [31]. Even though miscanthus is suitable for use in lightweight concretes [32], limited literature covers the potential of miscanthus concretes [33–35]. This paper proposes an environmental assessment of miscanthus lightweight blocks in the UK, and their potential application in conventional wall systems.

Low energy designs involve the investment in insulation of building's fabric, glazing and airtightness. These strategies could be eventually applied using insulating materials that are environmentally friendly, capable of reducing both the operational and embodied energy balance of dwellings. The aim of this paper is to assess the environmental performance of a composite lightweight material produced using local miscanthus shives. The study presents a comparative analysis of wall assembly systems made of typical standard materials used in the UK against those made of miscanthus-lime composites. The environmental performance of miscanthus-lime blocks wall was compared to that of the existing walling systems, providing quantitative evidence to support this technique within the construction industry, and thus the widespread implementation of miscanthus-based building materials in the UK. The environmental impacts are calculated for miscanthus concrete blocks and a sensitivity analysis was conducted to investigate the effect of the type of binder, the binder content level

and binder transport distances. In the end, the environmental impact indicators were analysed for wall assemblies that include miscanthus blocks and compared to a standard solid wall insulated with a layer of mineral wool.

2. System description and data inventory

2.1. Scope and description of system boundaries

In this study, a comparative LCA of wall systems was performed using the concept of life cycle analysis of building materials and component combinations (LCA-BMCC) as defined by Ortiz et al. [36]. The assessments were conducted from the extraction of raw materials to waste disposal/recycling, considering flows of materials and energy in separate subsystems: agricultural, processing and construction subsystems. An attributional life cycle approach (ALCA) that considers average data for all flows of different processes was used and results discussed at all levels of the overall system.

The framework, principles, and guidelines for life cycle assessments were followed as described within the International Organization for Standardization standards, ISO 14040 and ISO 14044. This paper presents an assessment of the environmental performance of miscanthus concrete and wall assemblies, from miscanthus grown in South West England. The overall system boundaries are presented in Fig. 1. The elements of the system in Fig. 1 were subdivided in subsystems as follows: (a) Miscanthus is grown at Lower Marsh farm in Taunton (Somerset), where elementary flows from soil preparation to miscanthus stems baling are considered. Miscanthus bales are then transported to factory site, chopped, dedusted and packaged. The details of the agricultural subsystem are presented in Fig. 2. (b) The chopped miscanthus shives are transported to the factory site where they are processed and mixed with binders to produce blocks. Fig. 3 shows the details of the blocks production subsystem. (c) The produced blocks are then transported to the building site where they are assembled and mounted in wall systems with clay bricks and concrete blocks. Fig. 4 illustrates the itinerary through processes of the aforementioned subsystems, from field at the farm to miscanthus blocks. A typical application of bio-based concrete in a traditional masonry wall assembly is shown in Fig. 5.

2.2. Inventory method and data collection

2.2.1. Cultivation of miscanthus and production of shiv

There is a variety of agricultural practices for miscanthus farming in the UK. However, the department for environment, food and rural affairs (DEFRA) has set a standard guide of best practices followed by most farmers to grow miscanthus. These practices were considered in addition to farming and crop management techniques in use at Lower Marsh farm in Taunton. The cultivation of miscanthus consists of several steps: field preparation or ploughing, rhizome planting, crop management and weed control; all occurring during the first year of crop establishment. The annual operations consist of harvesting, baling, transportation from field to the storage shed and shredding/chopping

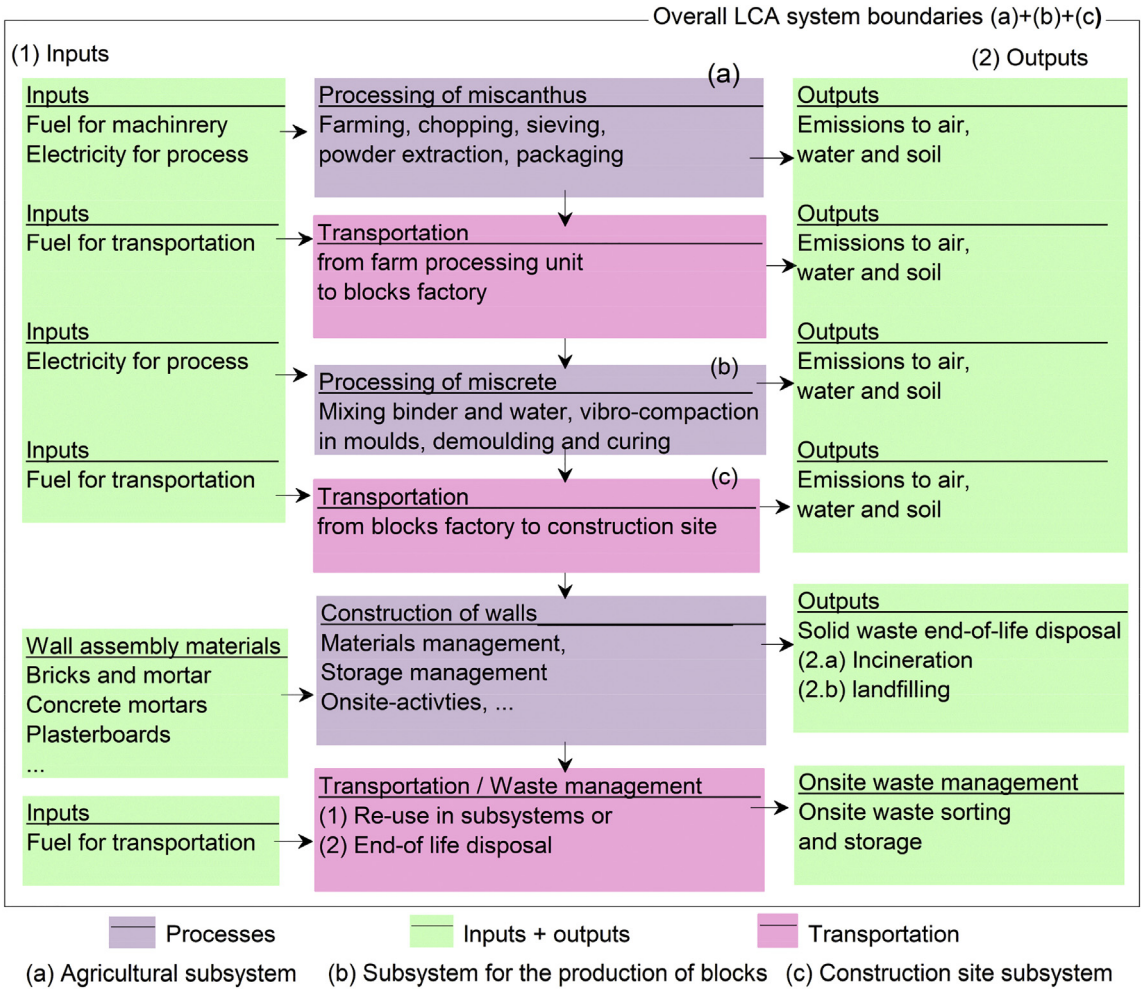

Fig. 1. Life cycle assessment boundaries for the overall miscanthus concrete walls environmental impact evaluation.

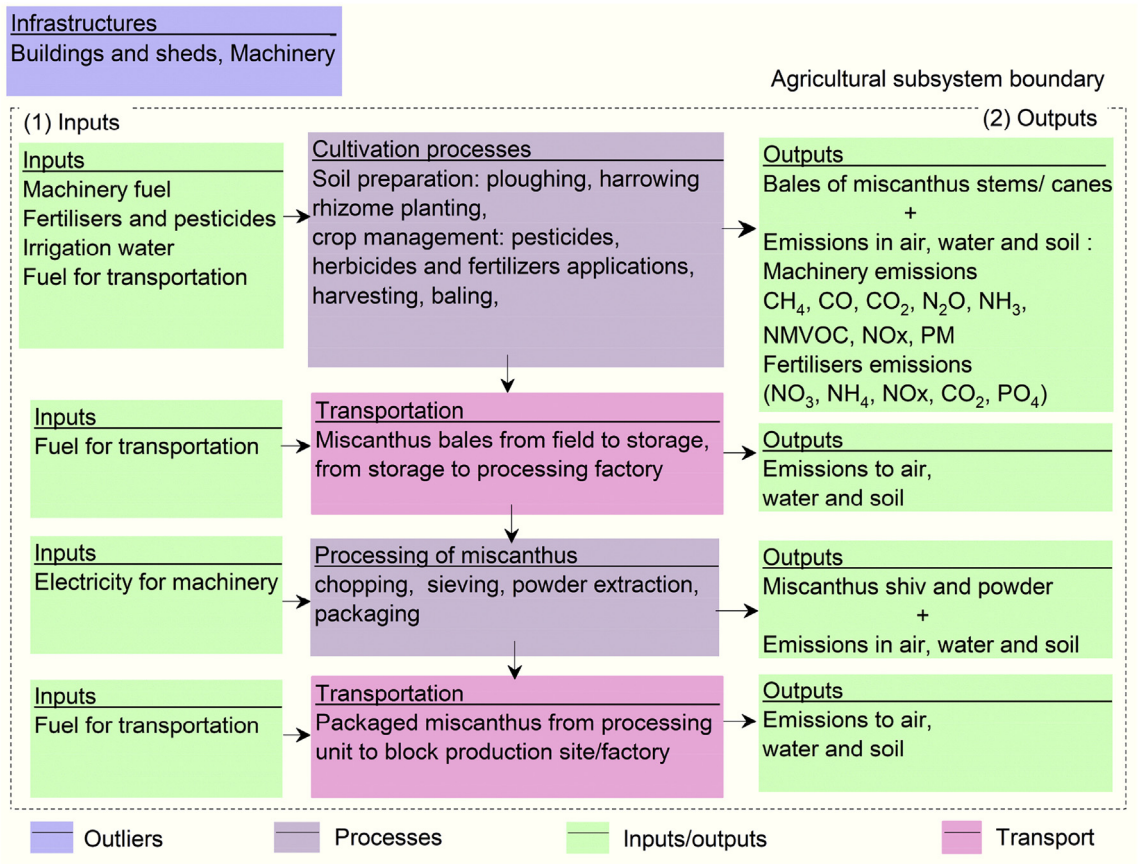

Fig. 2. The boundaries of the agricultural subsystem for the production of miscanthus shives.

of miscanthus canes. The average diesel consumption of agricultural machinery for all activities from ploughing to baling was obtained from data collected during a farm visit in Taunton. The total amount of diesel consumption was estimated at 88.5 l/ha for a complete agricultural cycle including ploughing, spraying of glyphosate and rhizome planting performed once every 20 years. A similar lifetime period was recorded in literature for miscanthus [37]. The production and supply of miscanthus rhizomes were not considered in the assessments. The impact of the agricultural subsystem processes was calculated on the basis of the performance of agricultural machinery in terms of power rate (hp), productivity (hours/ha), diesel consumption (l/ha) and emissions. There are no fertilizers applied in the farming of miscanthus at Lower Marsh farm. The application of glyphosate (3 kg/ha) was considered during the establishment year for weed control. Although a rather comprehensive analysis of processes was conducted, the life cycle assessments involving agricultural systems remain relatively complex. They require the evaluation of specific pedo-climatic conditions, farming management practices and technologies, specific characteristics of perennial crops and any actual crop rotations [38]. Such elements are beyond the scope of the present paper and were not considered.

Bio-based building materials benefit from the absorption of CO_2 during the annual growth cycle of crops. However, the quantification of biogenic carbon capture and sequestration of crops remains a controversial subject mainly due to the complexity of dynamic flows within the soil-air-plant system [39]. In a study on the environmental costs of growing miscanthus in the UK [40], in addition to biogenic capture of CO_2, the soil organic capture (SOC) was estimated at ~0.98 t of carbon /ha/year. However, soil carbon capture was not accounted for in this study. The biogenic CO_2 capture of miscanthus was stoichiometrically calculated from the eq. 1:

$$Q_{CO2} = C_c C_f (\rho_w V_w / 1 + w) \quad (1)$$

where Q_{CO2} is the captured carbon dioxide at the moisture w (%), C_c is the molar mass ratio of carbon dioxide to carbon (44/12), Cf the carbon fraction of the biomass (dry), ρ_w is the density of the biomass at w% moisture, V_w volume of the biomass at the moisture w%. This method is in accordance with EN 26449 standard and it is recommended by the Royal Institution of Charted Surveyors (RICS). The application of the eq. 1 gives a value of ~1.75 $kgCO_2$/ kg of miscanthus that was assigned to miscanthus shives in the LCA model as a negative CO_2 emission. An average annual yield of 10 t/ha was considered, and the mass allocation method was used for the products of miscanthus canes shredding: 80% of shives, 10% of fibres and 10% of dust. The production of miscanthus shives is performed in four major steps including bales opening, decortication of canes, separation of shives and fibres, and air-dedusting. This production line includes a tub grinder and a hammermill with 220 kWh of electric energy consumption for a processing capacity of 3.6 t per hour.

2.2.2. Mineral binders and production of miscanthus blocks

The most prevalent binder formulations used with bio-aggregates are widely reported in literature and consist of hydrated lime, hydraulic lime, and some of the common pozzolans. The binders used in the production of miscanthus concrete were a binary blend of hydrated lime (CL90s) and natural hydraulic lime (NHL3.5). Additional mineral pozzolans were considered, including ground granulated blast furnace slag (GGBS), fly ash (FA) and Ordinary Portland Cement (OPC). Hydrated lime, hydraulic lime and cement were sourced from Blue Circle. A number of lime and cement factories are available within 200 km distance

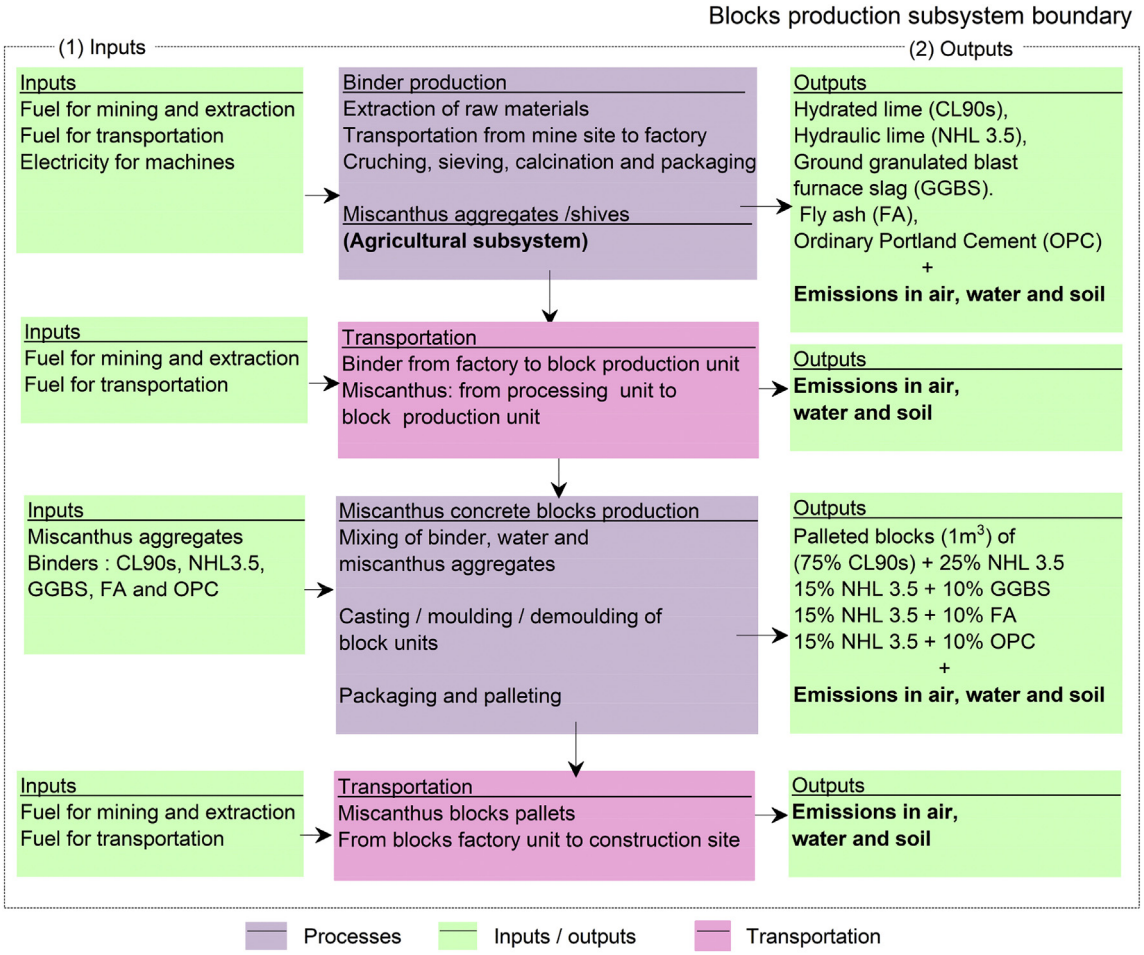

Fig. 3. The subsystem boundaries for the production of miscanthus concrete blocks.

around Somerset. Ground granulated blast furnace slag (GGBS) is a by-product of iron and steel production processes. It was sourced from Ecocem (Ireland). Its transportation distance was estimated at 557 km with 126 km of ferry across the Irish sea. Fly ash (FA) is a waste material produced during the combustion process in coal-fired power stations. It is a silico-aluminous material and presents high reactivity with free portlandite. Fly ash was sourced from a power plant in north Yorkshire (Drax power station) within an average distance estimated at ~450 km. The transportation of mineral pozzolans was performed by road and assumed within a 90% loaded 24-t truck for specific distances from suppliers.

The delivery of materials to the factory site for the production of miscanthus blocks was considered in 24 t freight lorries within distances of 100 km for miscanthus shives and 200 km for lime. The binder and miscanthus shives were mixed and cast using a typical concrete blocks production line that consumes 3.0 kWh/m^3 of mixture. The produced miscanthus blocks were subsequently cured on shelves and allowed to harden in indoor conditions with temperature and relative humidity ~20 °C and 50%RH. After curing, miscanthus blocks were packaged and transported to the construction site. It was assumed that the packaging required the use polyethylene films (100 g/m^2) and palletizing (1 pallet per m^3). The transportation from blocks production factory to the construction site was assumed within a distance of 100 km.

At the construction site, miscanthus concrete blocks were assembled with other building materials to constitute layered wall structures. The use phase of construction materials was considered after blocks were delivered on the building site and assembled in walls. In literature, different methods have been used to quantify the absorption of CO_2 for lime-based binders in lightweight hemp-based materials. Boutin et al. considered 0.249 kg CO_2/ kg binder [25], while Ip and Miller considered 0.571 kg CO_2/ kg binder [41]. Pretot et al. [42] and Arrigoni et al. [26] estimated the CO_2 uptake of hemp concrete at 0.325 and 0.462 kg CO_2/ kg of binder, respectively. In this study, the carbonation of lime-based binders was considered for hydraulic and hydrated lime at 0.514 kg CO_2 per kg lime, corresponding to the reabsorption of 90% of the CO_2 emitted during the calcination of limestone [43]. The assemblage of construction materials at the construction site requires a set of small tools and human energy that were not accounted for in the life cycle model. The production and supply of other construction materials were considered expect for those with <1 wt% (nails, wall ties). The end-of-life phase was considered for materials through waste transportation and treatment at municipal incineration centre or landfilling.

3. Methodology

3.1. Functional unit

The building regulation codes specify the requirements on heat transfer, air leakage and moisture condensation control in building fabrics and wall systems separating outdoor and indoor spaces. In this study, the functional unit of wall systems was chosen to comply with the energy performance requirements of the UK building regulations

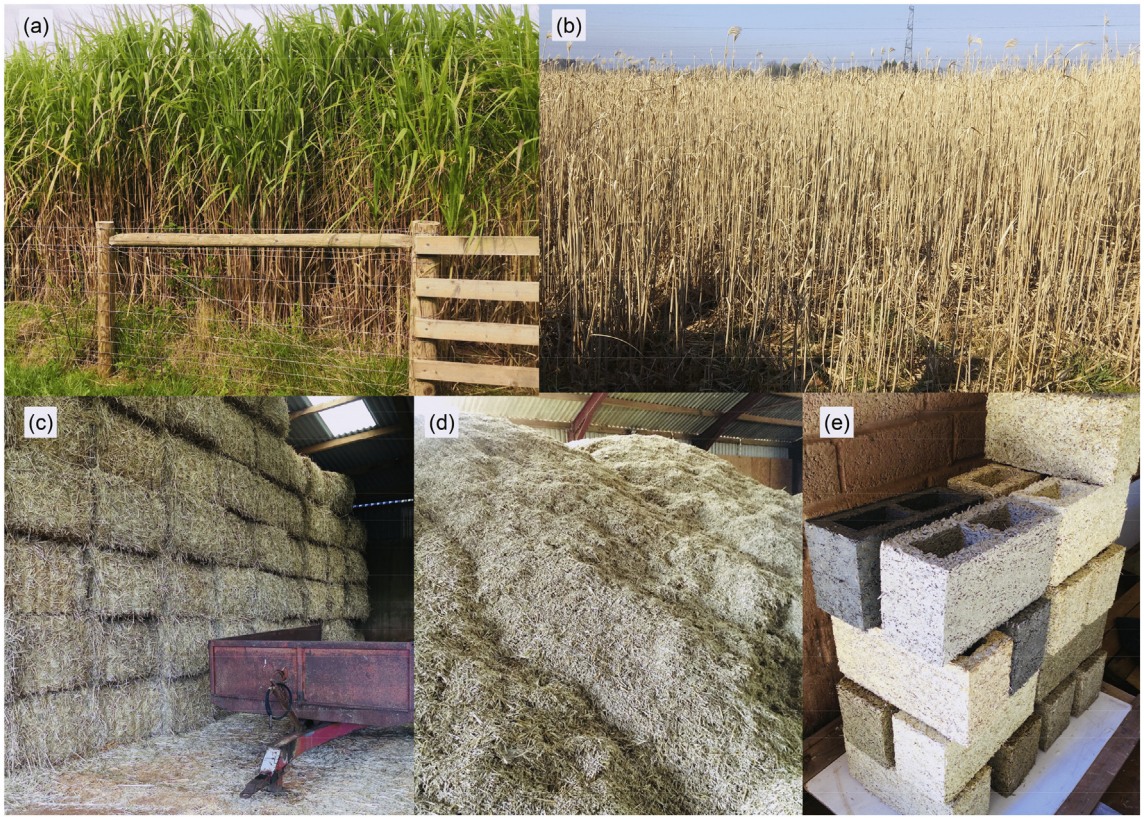

Fig. 4. Miscanthus block production: a) miscanthus field at Lower Marsh farm in Taunton, September 2019, b) senesced miscanthus canes, January 2020, c) Stacked bales of miscanthus canes, d) a pile of miscanthus shiv, e) typical miscanthus concrete blocks.

(Part L) [44]. To compare components, both wall systems made of conventional insulating materials and those made of miscanthus concrete were set to exhibit similar insulation performance. The functional unit was defined as one square metre of wall and the thickness of elements adjusted to have the same thermal transmittance value (U-value) of ~0.30 W/m^{2}K as prescribed in the UK building regulations standard (conservation of fuel and power, approved document L) and commonly used in the thermal calculations of buildings [45]. The wall systems were adapted from common practices in the construction of residential buildings in the South West of England as detailed in the documents from the Local Authority Building Control (LABC) [46]. All wall systems were assumed of the same external application and the insulation role considered the most essential. Other properties such as mechanical, moisture transport and durability were not considered. The structural performance of wall scenarios was assumed in accordance with the Approved document A of the UK building regulations. The thermal conductivity of miscanthus concrete was estimated from the model proposed by Cérézo: $\lambda_d = 0.0002\rho + 0.0194$ [47], with λ_d and ρ the effective thermal conductivity and dry density of blocks, respectively. This model agrees with experimental values reported by Nguyen, considering the anisotropy of hemp concretes [48]. Bio-based materials exhibit both conductive and radiative modes of heat transfer within their specific pore structure. The effective thermal conductivity was considered because conduction remains largely dominant and convection has been shown to be less seemingly existent in bio-based materials [49]. In this paper, considering miscanthus concrete with a density in the range of 450–550 kg/m^3, the effective thermal conductivity λ_d of 0.11–0.13 W/m.K was considered in the calculation of U-values. However, the variation of λ_d exhibited little effect on environmental impacts results and was not further investigated. Even though the thermal conductivity of bio-based concretes can considerably vary, it remains mostly in the range 0.05–0.20 W/m.K depending on their formulation [49].

Fig. 5. Illustration of a typical bio-based cavity wall assembly made of hemp concrete. (a) load bearing fired clay blocks, (b) layer of hemp concrete blocks and (c) outer leaf layer of bricks (Courtesy of Isohemp, 2020).

Three scenarios of different wall assemblies were investigated. Materials that make up these structures from the exterior to the interior were: (a) a traditional structural timber frame filled with miscanthus concrete and cladded with 4 mm slates on wood battens, 12.5 mm of

OSB sheathing board, 400 mm of miscanthus concrete and 12.5 mm of plaster board (WSA–Ti). (b) A cavity wall made of a 102 mm brick layer, 50 mm air cavity, a breather membrane, 9 mm of OSB sheathing board, 250 mm of miscanthus concrete, a vapour control layer and 12.5 mmm of plasterboard (WSA–Br) and (c) a solid wall made of 102 mm brick layer, a breather membrane, 85 mm of rock wool, 100 mm of autoclaved aerated concrete blocks, a vapour control layer and 12.5 mm of plaster board (WSS-Min.W). Fig. 6 shows the detailed structural composition of analysed scenarios of wall structures and Table 1 details the elementary fluxes in the functional unit of 1 m^2 for all wall scenarios. The thermal properties of these materials were obtained from the environmental product declarations (EPD) of available products on the UK market and the thicknesses of the walls elements adjusted for an overall thermal transmittance U-value of 0.30 W/m^2K for all scenarios. The final Req. value for all wall scenarios is 3.35, considering external and internal thermal resistances (Rse and Rsi) of 0.04 and 0.13 m^2K/W, respectively.

3.2. Emissions models and impact indicators

The quantification of flows in the agricultural subsystem requires data or models for fuel consumption, exhaust gases and direct emissions in air, soil, and water. There exist a wide range of available models to estimate fuel consumption from farming operations. Andrianadraina et al. used a combination of fuel consumption and engine emissions models for hemp farming operations and integrated them in hemp concrete LCA [50]. In this study, fuel consumption data was acquired at Lower Marsh Farm in Taunton (UK) and complied with models in [51]. However, the emission of pollutants (CH_4, CO, CO_2, N_2O, NH_3, NMVOC, NOx, PM) (kg/ha) was modelled using the eq. 2:

$$E_i = \sum_{j,t} FC_{j,t} \times EF_{i,j,t} \quad (2)$$

where $FC_{j,t}$ is fuel consumption for a fuel type j by an equipment of technology type t (L/ha) and $EF_{i,j,t}$ is the average emission factor for a pollutant i, from a fuel type j and an equipment of technology type t.

The method in eq. 2 is recommended in the EU and builds on the methodology from the US Environment Protection Agency (EPA) designed to estimate off-road emissions, which has been enacted in the UK. The methods used to estimate exhaust gas emissions from agricultural tractors is compliant with methodologies proposed in literature [52]. Soil carbon impacts are reported in agriculture literature, yet they remain considered uncertain among CO_2 removal strategies [53]. The soil organic carbon sequestration can reach significant levels depending on agricultural practices. Nakajima et al. reported soil carbon sequestration of 1.96 ± 0.82 Mg C/ha/year for miscanthus [54]. However, these results remain site specific and highly influenced by the type of climate, the site use history and soil management practices in place. Considering the uncertainties related to the evolution of agricultural practices and site history data, soil carbon capture and storage was not considered in the model.

There exist a variety of LCA softwares including SimaPro [55], GaBi [56], Umberto [57], Quantis [58], OpenLCA [59]. The software OpenLCA v1.7.4 developed by GreenDelta was used in conjunction with Ecoinvent 3_1 database. It allows to design a modular object-oriented LCA models in a highly flexible and opensource environment [60]. The obtained results were exported and analysed using Excel. The impact assessment methods can be classified as midpoints and endpoints methods. The midpoints method was chosen in this study as it restricts the interpretation of quantitative results at the early stages of cause-effects chain, which limits the uncertainties associated with grouping into end-point categories. At the LCIA stage, impacts were calculated based on CML (baseline) v 4.4-January 2015 method developed by the Institute of Environmental Sciences (CML) at the University of Leiden, Netherland. It provides results in terms of 11 impact categories: acidification potential (Ac·P), climate change or global warming potential (GWP100), depletion of abiotic resources - elements, ultimate reserves (DAR-elements), depletion of abiotic resources - fossil fuels (DAR-fossils), eutrophication potential (Eu·P), freshwater aquatic ecotoxicity potential (FAETP), human toxicity potential (HTP), marine aquatic ecotoxicity potential (MAETP), ozone layer depletion potential (ODP), photochemical oxidation (Ph.O) and terrestrial ecotoxicity potential (TETP). Some assumptions and hypotheses were considered throughout the assessment stages:

- The potential environmental impacts associated with the construction of agricultural buildings and the manufacturing of machinery were not considered in the model.

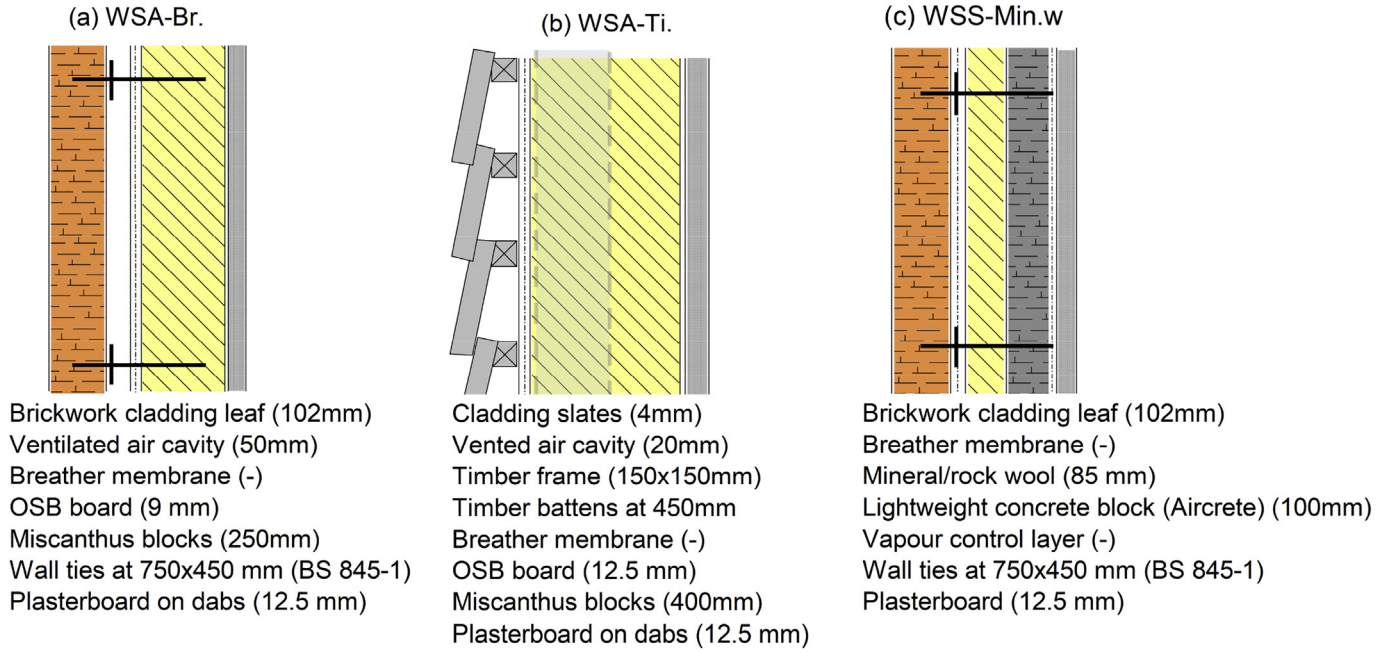

Fig. 6. The schematic structure of wall assemblies' scenarios. From left (exterior) to right (interior) (elements not on scale).

Table 1
Elementary fluxes related to the functional units of wall assemblies' scenarios (kg/FU). The composition of miscrete (miscanthus concrete) as per scenario A(R) in Table 2.

Scenario	Brickwork (1)	Miscrete (2)	Timber	Slates	OSB (3)	Aircrete	Plasterboard	Mineral wool
WSA-Br	257	137.5	0.0	0.0	5.4	0.0	8.0	0.0
WSA-Ti	0.0	220.0	13.5	6.8	5.4	0.0	8.0	0.0
WSS-Min.w	257	0.0	0.0	0.0	0.0	53.0	8.0	3.8

(1) Brickwork as per BS EN 771–1;(2) miscrete density at 550 kg/m^3, (3) OSB: Oriented Strand Board

- Components of less than 1 wt% of the total inventory and data of high uncertainty (wall ties, nails for wood frame, …) were excluded from the model.
- The electricity for wood frame mounting was estimated negligible and hence not considered.
- The method used in the assessments is cradle to grave and a life duration of 50 years for wall systems and their components was assumed. Structural systems were assumed to last for 100 years.

3.3. Results analysis and optimisation

The obtained results were normalized to the maximum values of impact categories to assess the variations within individual impact categories for all scenarios. Linear programming (LP) approach was used for comparative assessment of scenarios for the overall environmental performance considering all the 11 impact categories. The computer software LINGO 18.0 was used to solve the optimisation linear programming (LP) model [61]. An LP model (eq. 3) can be described as an optimisation (minimisation) of a series objective functions applied to impact categories [62]: Minimize $Q_i(x)$;

$$Q_i(x) = \sum_{k=1}^{l} a_{ki}x_{ki} = a_{1i}x_{1i} + a_{2i}x_{2i} + \ldots + a_{li}x_{li} \quad (3)$$

where $Q_i(x)$ is the i-th objective function, a_{ki} the coefficient of the objective function and x_i the quantitative measures of outputs which is subject to specific constraints. In the context of LCA, the objective functions can represent the overall environmental impact where a_{ki} represents the relative contribution of a burden or impact indicator x_i [63]. In this study, the linear weighted sum method was the approach adopted to solve the problem in eq. 4, and the eq. 3 became: Minimize $f(x)$;

$$f(x) = \sum_{k=1}^{l} \omega_k Q_k^o(x) = \omega_1 Q_1^o(x) + \omega_2 Q_2^o(x) + \ldots + \omega_l Q_l^o(x) \quad (4)$$

where the $Q_k^o(x)$ is the normalized objective function of $Q_k(x)$ and ω_k represents weighting factors such that $\omega_1 + \omega_2 + \ldots + \omega_l = 1$.

4. Results and discussions

In this section, the environmental impact categories are reported for both miscanthus concrete blocks and wall assembly scenarios. Three scenarios were considered for miscanthus blocks to investigate the sensitivity of the model and optimize the environmental performance of blocks. 'Binder content' scenarios investigate the effects of increasing levels of binder to aggregate weight ratios: low binder content (1.5 b/a), reference binder content (2.0 b/a), medium binder content (2.5 b/a) and high binder content (3.0 b/a). 'Composition of binder blends' scenarios consider a binary binder made of 75% hydrated lime +25% hydraulic lime (75%CL90s + 25%NHL3.5) and three ternary binders where the main components are 75% hydrated lime and 15% hydraulic lime, and 10% ground granulated blast furnace slag (GGBS), fly ash (FA) or cement (OPC): 75%CL90s + 15%NHL3.5 + 10%GGBS/10% FA/10%OPC, respectively. GGBS and FA are industrial wastes that are widely available in the UK, and potentially beneficial from both environmental and early age strength improvement standpoints. Last, the impact of transportation distance of binders was evaluated at three levels: low distance (100 km), reference distance (200 km) and long distance (500 km). Two extreme distances were added to assess the overall sensitivity of the model to freight distances: (a) very short distance (10 km) and (b) very long distance (2000 km). The details of these scenarios are shown in Table 2.

4.1. Miscanthus concrete blocks: base case results

The results were first presented for all impacts categories for miscanthus concrete base case (scenario A), followed by a description of the contributions from the main production phases (agricultural phase, miscanthus blocks production and transportation). A detailed analysis of global warming potential from the base case is presented, followed by a sensitivity analysis of the LCA model where the type of binder, the binder content and binder transportation distances were considered as variable parameters. The results from sensitivity analysis related to the type of binders and binder content levels were subsequently used to optimize the environmental performance of the miscanthus concrete using Linear Programming in section 4.2.2.

The breakdown of GWP100 from processes related to the production of miscanthus concrete blocks base case (scenario A) is presented in Fig. 7a and b. Detailed results for all impact categories and a breakdown of GWP100 are presented in Tables 3 and 4, respectively. In fact, the production of hydrated lime involves the emission of 0.75kgCO_2eq /kg of produced lime [64]. The recorded absorption of carbon dioxide attributed to the production of miscanthus shives was due to a high biogenic CO_2 absorption inflow of −1.75 kgCO_2eq/kg of miscanthus shives. The reported results show that the production of binders and their transportation contribute to ~239.89 kgCO_2eq/m^3 while miscanthus aggregates absorb ~ −276.16 kgCO_2eq/m^3. In all, the carbon footprint of binders is estimated at 0.76 kg CO_2eq./kg of binder. These figures suggest that the optimisation of GWP100 impact level requires mix design methods involving a reduction of binder content and an increase of miscanthus aggregate content. The overall net global warming potential of miscanthus concrete is −134.74 kgCO_2eq/m^3. The major contributor remains the production of binders which accounts for 167.50 and 58.99 kg CO_2eq/m^3 for CL90s and NHL3.5, respectively, for a total of 226.49 KgCO_2eq/m^3. The carbonation of miscanthus blocks over the life cycle contributed for −161.96 kgCO_2eq/m^3.

Table 5 summarises all levels of impact categories recorded for miscanthus concrete base scenario A. These results were compared to literature values for hemp concrete studies that used CML as LCIA method. Not all impact categories were considered in these studies as specified in the NF P01-010 and EN 15804:2012 standards. Fig. 8 shows the cumulative contribution of miscanthus shives production, blocks casting, transportation, and use phase of miscanthus blocks for all impact indicators. These results highlight that the production of blocks contributes for at least 70% to all impact categories and exceptionally for the GWP (~105%). The highest values of impact categories were recorded for photochemical oxidation (Ph.O), acidification potential (Ac·P) and eutrophication potential (Eu·P), all reaching at least

Table 2
Miscanthus concrete production and transportation scenarios.

Scenario	Variable	b/a	Binder type / composition	Misc	Water	Binder	T.D. Misc	T.D Binder
	Parameters	(kg/kg)		(kg/m^3)	(kg/m^3)	(kg/m^3)	(km)	(km)
A (R)	Type of binder	2.0	CL90s + NHL3.5 (i)	157	348.17	315.1	100	200
B		2.0	CL90s + NHL3.5 + GGBS (ii)	157	348.17	315.1	100	200
C		2.0	CL90s + NHL3.5 + FA (ii)	157	348.17	315.1	100	200
D		2.0	CL90s + NHL3.5 + OPC (ii)	157	348.17	315.1	100	200
A-1.5 kb	Binder content	1.5	CL90s + NHL3.5 (ii)	187	358.12	277.3	100	200
A-2.0 kb (R)		2	CL90s + NHL3.5 (i)	157	348.17	315.1	100	200
A-2.5 kb		2.5	CL90s + NHL3.5 (i)	137.14	340.8	342.86	100	200
A-3.0 kb		3	CL90s + NHL3.5 (i)	121.42	335.12	364.25	100	200
A-2.15 kb-T1 (R)	Transport distances	2.0	CL90s + NHL3.5 (i)	157	348.17	315.1	100	200
A-2.15 kb-T2		2.0	CL90s + NHL3.5 (i)	157	348.17	315.1	100	100
A-2.15 kb-T3		2.0	CL90s + NHL3.5 (i)	157	348.17	315.1	100	50
A-2.15 kb-VL		2.0	CL90s + NHL3.5 (i)	157	348.17	315.1	100	2000
A-2.15 kb-VS		2	CL90s + NHL3.5 (i)	157	348.17	315.1	100	10

b/a: Binder to aggregate ratio; TD: Transportation distance; Misc: Miscanthus shiv.
(i) 75% hydrated lime [CL90s] + 25% natural hydraulic lime [NHL3.5]; (ii) 75% hydrated lime [CL90s] + 15% natural hydraulic lime [NHL3.5] + 10% mineral additions.
Mineral additions: (GGBS, ground granulated blast furnace slag; OPC, Ordinary Portland Cement, FA: fly ash).
(R), The base case as reference for every set of scenarios within a type of studied variable parameter.

~87% contribution. These are related to high-energy extraction and processing of raw materials, transportation, and their associated emissions to air, water, and soil.

4.2. Sensitivity analysis for the base case scenario

The sensitivity analysis was performed to study the effects of uncertainties and variable data on the robustness of the LCA model. In this study, the sensitivity of the LCA was investigated considering the binder type, binder content and transportation distances. However, different impact categories were quantified in different units and to compare scenarios, an internal normalization was applied with 100% value attributed to the highest value from any scenario within each impact category.

4.2.1. Miscanthus concrete blocks: Effect of binder composition and binder content

The sensitivity of the LCA model for miscanthus concrete was investigated at the concrete composition level on two factors: the type of binder and binder content. The types of binders that compose binary and ternary blends were hydrated lime, hydraulic lime and pozzolanic materials as shown in Table 2. The variation of binder type and content might incur modifications in the overall mechanical strength and thermal performance of the composites. These impacts were not considered in this paper. Fig. 9 shows the variation of impact categories values as a function of binder content levels in miscanthus concrete. The variations of levels of impact categories scale with binder content levels. However, GWP 100 recorded the highest impact variation (~72.7%) as direct emissions are cut down by the reduction of binder content and biogenic CO_2 capture increased by the increased miscanthus content. All other impact levels vary in the range of 10.40% to 21% with the lowest and highest variations recorded for DAR-elements and Ph.O, respectively.

Fig. 10 presents the variation of environmental impact categories versus the types of binders. All binders are made of 75% hydrated (calcic) lime and varying compositions as shown in Table 2. In general, the incorporation of mineral additions in the binder blends has resulted in reductions for all impact categories with the highest reductions recorded for 75%CL90s + 15%NHL3.5 + 10% GGBS and 10% FA (scenarios B and C). The minimum reductions across all impact categories among all the investigated mineral additions correspond to the binder blend containing 10% OPC. The scenario D specifically exhibited the highest values for GWP 100 corresponding to −118.56 kg CO_2eq./m^3 compared to −147.23 kg CO_2eq./m^3 for scenario B. This is because the production of cement and lime is highly energy-intensive, while GGBS is an industrial waste with lower energy consumption (1300 MJ/t GGBS and 5000 MJ/t OPC) and a large part of its production CO_2 allocated to the main products, iron and steel [65]. The high values related to water and soil pollutions for scenarios A and D can be attributed to high values of water consumption and pollution associated with lime and cement production, especially containing pollutants such as Cadmium and/or Mercury [66]. However, the variations of impact categories values related to type mineral additions remain low for most of impact categories

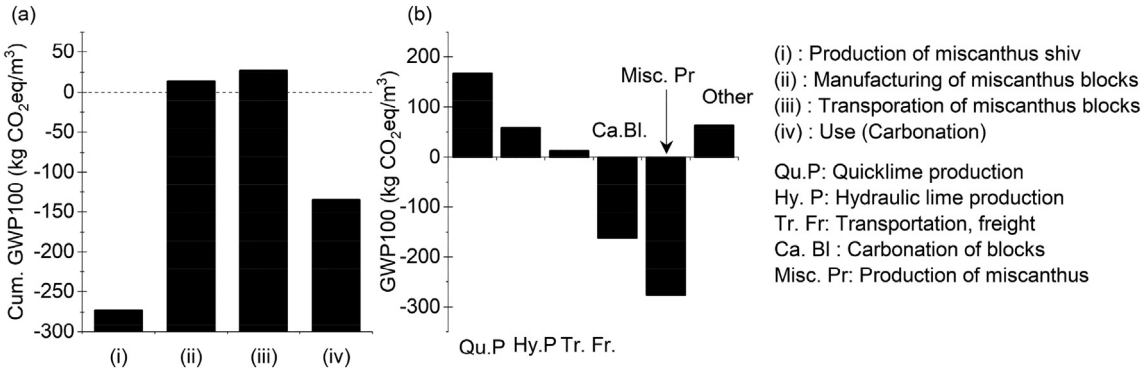

Fig. 7. Impact of miscanthus concrete, scenario A, on global warming potential (GWP100). (a) The cumulative carbon balance after the end of major phases of miscanthus blocks life cycle; (b) the individual contribution of major processes at 1% cut-off.

Table 3
Cumulative impact levels for steps of the production of miscanthus concrete (Scenario A). Step 0 presents impact levels for the agricultural and processing subsystems, production of 157 kg of miscanthus shiv; step 1: the production of miscanthus blocks (1 m^3); step 2: the transportation of miscanthus blocks from the manufacturing factory to building site; step 3: the carbonation of miscanthus block during the lifecycle (100 years).

Impact category	Abbreviation	Units	Step 0	Step 1	Step 2	Step 3
Acidification potential - average Europe	Ac·P	kg SO_2 eq.	1.91E-02	5.69E-01	6.16E-01	6.16E-01
Climate change - GWP100	GWP 100	kg CO_2 eq.	-2.73E+02	1.35E+01	2.72E+01	-1.35E+02
Depletion of abiotic resources - elements, ultimate reserves	DAR-Elements	kg Sb eq.	9.65E-06	1.10E-04	1.54E-04	1.54E-04
Depletion of abiotic resources - fossil fuels	DAR-Fossils	MJ	6.98E+01	1.79E+03	1.99E+03	1.99E+03
Eutrophication – generic	Eu·P	kg PO_4--- eq.	5.93E-03	1.20E-01	1.29E-01	1.29E-01
Freshwater aquatic ecotoxicity - FAETP inf	FAETP	kg 1,4-DCB eq.	1.27E+00	1.48E+01	1.65E+01	1.65E+01
Human toxicity - HTP inf	HTP	kg 1,4-DCB eq.	1.49E+00	4.39E+01	5.08E+01	5.08E+01
Marine aquatic ecotoxicity - MAETP inf	MAETP	kg 1,4-DCB eq.	4.26E+03	5.09E+04	5.53E+04	5.53E+04
Ozone layer depletion - ODP steady state	ODP	kg CFC-11 eq.	7.15E-07	1.96E-05	2.21E-05	2.21E-05
Photochemical oxidation - high Nox	Ph.O	kg C_2H_4 eq.	1.09E-03	4.94E-02	5.18E-02	5.18E-02
Terrestrial ecotoxicity - TETP inf	TETP	kg 1,4-DCB eq.	2.68E-02	4.22E-01	4.69E-01	4.69E-01

Table 4
The GWP100 breakdown for major processes of the production of 1 m^3 miscanthus concrete (Scenario A).

Major processes at 1% cut-off	GWP100 (kg CO_2eq./m^3)
Quicklime production, in pieces, loose	167.50
Lime production, hydraulic	58.99
Transport, freight, lorry 24 t (90% loaded)	13.40
Miscanthus Blocks Use - Carbonation (MSA-1)	−161.96
Miscanthus shiv production (Taunton)	−276.16
Other	63.49

(4.5% to 11.5%), allowing a potential flexibility in the design of binary or ternary binder blends. The overall effect of binder type and content for miscanthus concrete is shown in Fig. 11. In general, the mix parameters that lead to the minimum levels for most impact categories are the reduction of binder content and the use of GGBS (scenarios B and 1.5 b). In the calculation of impacts, the economic allocation was considered for GGBS to take into consideration its 'iron/steel-production' by-product nature. Within the considered range of parameters, the most optimizable impacts are Ph.O and Eu·P, presenting the highest variations (>20%). A linear programming algorithm has been used in section 4.2.2 to find the optimal combination of mix-design parameters using LINGO (Linear Interactive and Discrete Optimiser).

4.2.2. Miscanthus concrete blocks – Optimization of binder content and binder type

The optimum mix design of miscanthus concrete composition can be identified using either qualitative or objective optimization methods. The results for qualitative analysis using a graphical approach are shown in Fig. 11 that is based on the normalized data from the actual values of impact categories. Although the results are quite clear for each individual impact category, it remains difficult to assess the overall performance that considers all impact categories. For such multiple objective functions, mathematical modelling remains more reliable than qualitative analysis. Mathematical programming was used to highlight the best mix design among the eight mix design options using the software package LINGO. Objective functions were composed of selected impact categories out of the CML baseline normalized results by applying weighting factors. While the external normalization remains the most prevalent in comparative LCAs, there is a substantial risk for the results being driven by the external reference values rather than the actual values from scenarios [67]. In this study, the internal normalization of impact categories values was preferred and performed using the eq. 5:

$$Q_k^0 = 1 - (\max Q_{ij} - Q_{ij}) / \max Q_{ij} \quad (5)$$

where Q_k^0 is the internally normalized results and Qij is the initial impact category value.

The Q_k^0 values were then weighted with ω_k coefficients and incorporated in the eq. 4. Different weighting methods in LCA have been developed and applied to results obtained using different LCIA methods. For instance, Castellani et al. developed a weighting method applicable to ILCD method derived results [68]. Based on the aforementioned study, ILCD compliant weighting sets that aim at various environmental perspectives were proposed in the European guide for interpreting life cycle assessment results [69]. However, weighting remains an optional LCA step for which no CML-compliant weighting method has been proposed [70]. In this study, weighting factors were adapted ILCD-compliant methods and weighting coefficients from similar and/or related impact categories re-adjusted from original values as presented

Table 5
Environmental impact categories levels for base case scenario of 1m^3 of miscanthus concrete (scenario A). The values were compared to literature data recalculated for 1 m^3 of hemp concrete. NA (Not Available) indicates that values for these impact categories were not reported. In Arrigoni et al. the values are the minima of all scenarios. The maximum values are shown in parentheses. DCB = Dichlorobenzene.

		Present study	Boutin et al. [25]	Arrigoni et al. [26]
Impact categories	Units	Impact category levels per m^3		
TETP	kg 1,4-DCB eq.	0.469	NA	NA
Eu.P	kg PO_4--- eq.	0.129	NA	5.28E-02(7.06E-02)
GWP 100	kg CO_2 eq.	−134.743	−136.68	- 40 (−140)
Ac·P	kg SO_2 eq.	0.616	0.385	0.3 (0.6)
HTP	kg 1,4- DCB eq.	50.760	NA	NA
ODP	kg CFC-11 eq.	2.21E-05	3.85E-05	1.44E-05(1.88E-05)
Ph.O	kg C_2H_4eq.	5.18E-02	2.08E-02	2.24E-02(3.27E-02)
DAR-Elements	kg Sb eq.	1.50E-04	5.01E-01	6.92E-06(1.45E-01)
DAR-Fossils	MJ	1993.65	1517.67	1330(1607)
MAETP	kg 1,4-DCB eq.	55,272.60	NA	NA
FAETP	kg 1,4-DCB eq.	16.53	NA	NA

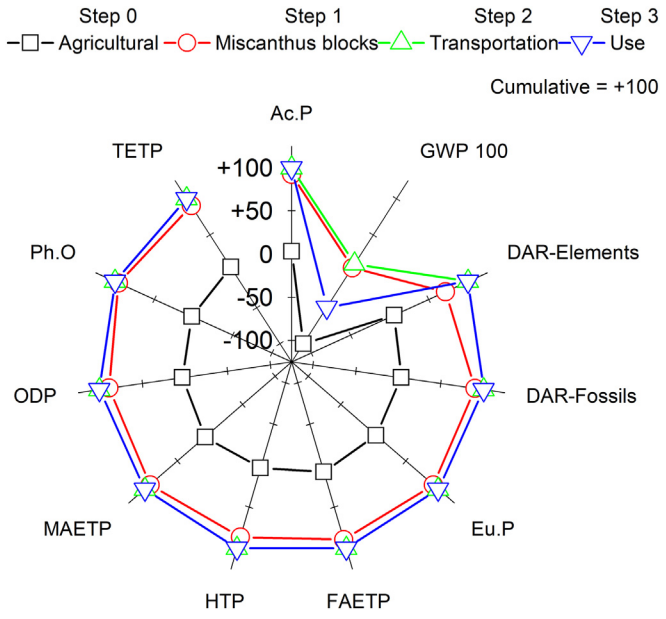

Fig. 8. Cumulative contribution to environmental impacts for major steps in the production of 1m^3 miscanthus blocks 100% represent the maximum value within each impact category through the processes of the production steps (0) to (3).

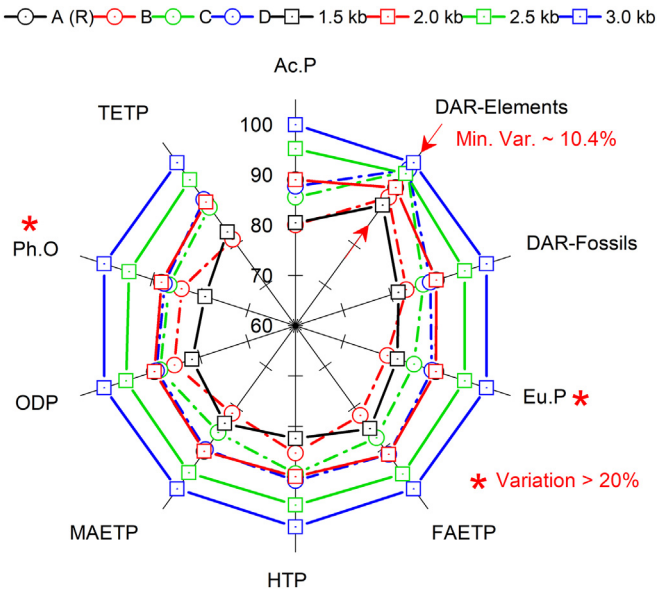

Fig. 11. Effect of binder content and type of binder on environmental impacts for 1 m^3 of miscanthus concrete blocks. Results were normalized on the maximum values within impact categories for all scenarios.

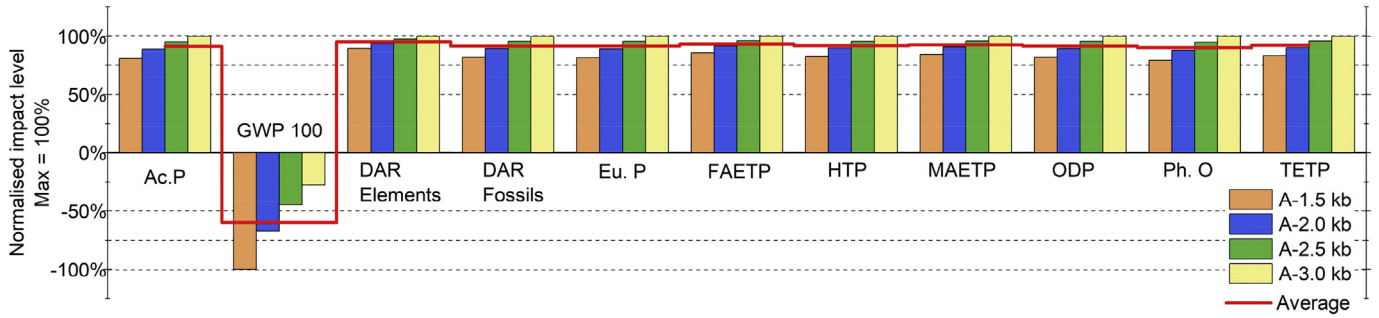

Fig. 9. Effect of binder content on environmental impacts for 1 m3 of miscanthus concrete blocks – binder to aggregate ratio levels (b/a) of 1.5, 2.0 (reference), 2.5 and 3.0. For each indicator, the maximum result was set at 100% and the results of the other variants are displayed in relation to this result.

in Table 6. The best mix designs were scenarios B (75%CL90s + 15% NHL3.5 + 10% GGBS) and A-1.5 (b/a) considering binder composition and binder content, respectively.

4.2.3. Miscanthus concrete blocks – Effect of binder transportation distances

Considering regional sourcing of miscanthus shives, transportation of binders is the second contributor to the GWP100 and could eventually influence other environmental parameters. The sensitivity of the LCA model of miscanthus concrete blocks was investigated for eventual transportation distances of 50 km, 100 km and 200 km. Extreme distances (very short distance: 10 km and very long distance: 2000 km) were included in the sensitivity analysis of the LCA model. Fig. 12 shows the variation of levels of impact categories versus binder transportation distances. The recorded results were normalized to the

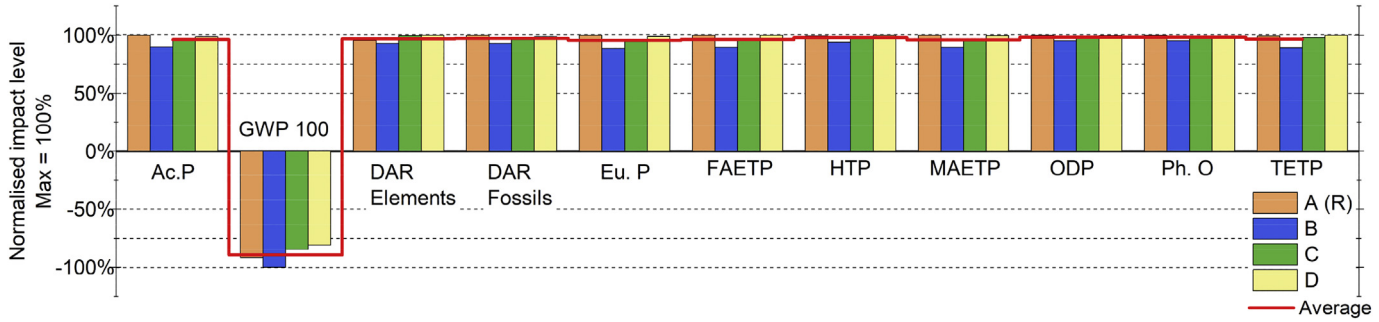

Fig. 10. Effect of type of binder on environmental impacts for 1 m^3 of miscanthus concrete blocks. All binder blends were based on 75 wt% of hydrated lime (CL90s).

Table 6
Optimization of miscanthus concrete by mathematical linear programming. The values of weights were considered as coefficients ω_k in the eq. 4 and applied in LINGO. The constraint is that all impact category values are at least less than average values.

Weighting perspective	AcP	GWP100	DAR-El	DAR Foss	EuP	FAETP	HTP	MAETP	ODP	Ph.O	TETP
Distance to policy target (a)	9.9	9.6	8.6	8.0	9.5	8.6	9.4	8.6	8.9	10.3	8.6
Distance to planetary boundaries (b)	4	28	/	/	10	12	/	5	4	32	5
Damage oriented (c)	4.6	42.0	12.1	12.1	/	/	7.6	/	/	/	21.6
Panel based (d)	5.2	24.2	7.9	7.9	5.9	11.9	11.5	3.3	4.6	6.4	11.2

(a) Distance to target for EU policies considering binding and nonbinding target for 2020 (Castellani et al. [68]).
(b) Considering planetary boundaries (Tuomisto et al. [71]; Bjørn and Hauschild, [72]).
(d) Relevance to midpoint indicators based on their contribution to impact at the endpoints (Sala et al. [73]).
(d) Resulting from the combination of different panel-based approaches (Huppes et al. [74]).

maximum impact indicator values among the investigated scenarios. Different impact categories were affected unevenly. The lowest effect was observed for photochemical oxidation with a variation of ~27% (transportation of distance range of 10 km – 2000 km) due to the fact that it remains related to the blocks production subsystem that is common among the investigated scenarios. The most affected impact categories recorded are DAR-elements and GWP 100 with variations >73%. This is due to a combination of the extraction and processing of diesel and transportation-related emissions. In general, the longer the transport distance, the higher the recorded environmental impacts.

4.3. Environmental performance of miscanthus concrete wall assemblies

In order to assess the environmental impact of miscanthus concrete used as an insulation material within typical wall systems against marketed insulation technologies, an impact analysis was carried out. Environmental impact results for the investigated wall structures were normalized to the maximum impact categories among the investigated wall structures: the base scenario is the timber-framed wall filled with miscanthus concrete (WSA–Ti). Other scenarios were considered where miscanthus concrete replaces the insulation in a typical cavity wall (WSA–Br.) and a standard solid wall insulated with mineral wool (WSS-Min.w). The energy and materials flows associated with the construction activities and onsite assemblies is negligible compared to the energy inputs from materials production and supply. Hence, no further breakdown of processes beyond materials production and supply was performed. The impact category levels for the wall assemblies, as reported in Table 7, show that the most noticeable impact categories for WSA-Ti scenario are GWP100 (−97.3 $kgCO_2eq./f.u$), and the depletion of abiotic resources (~982 MJ/f.u) which is mainly attributable to the production of diesel and gas used for the extraction, transportation, and processing of binders.

Fig. 13 compares the levels of environmental impacts categories for the investigated wall assembly scenarios. All the assessed impact categories levels remain the lowest for WSA-Ti wall scenario except for ODP, Ph.O and TETP. Compared to a typical standard wall assembly (WSS-Min. w), the levels of these impacts remain high for miscanthus concrete-based wall scenarios (WSA–Br. and WSA–Ti) and presumably originated from the agricultural subsystem processes and their associated emissions in soil. In all, the WSA–Br. exhibits the highest levels for most impact categories. This can be attributed to the high energy requirement (~700 kWh/t) for the firing of clayey materials at temperatures between 900 °C and 1150 °C [75]. However, GHG emissions from the WSA–Br. scenario were offset by the CO_2 absorption of miscanthus-lime blocks to a low net value of ~31.12 kg CO_2eq/f.u. The highest variation across wall assembly scenarios was recorded for GWP 100 with a 216% variation between WSA-Ti and WSS-Min.w while the lowest variation was obtained for FAETP with 1.31%. In general, comparing WSA–Br. and WSA-Ti revealed that the association of clay bricks outer leaf layer with miscanthus concrete in a wall structure offsets most of benefits from miscanthus concrete and leads to values of impact indicators even higher than those from WSA-Min.w for most impact categories. Still, the GWP100 from the WSA–Br. scenario remained ~84% lower than that from WSA-Min.w. Although associating bricks with miscanthus blocks results in net positive GHG emissions in new-build scenarios, the application remains plausible in retrofitting situations. In a similar study, in a retrofitting scenario of a Victorian houses' uninsulated brick walls using hemp concrete, Griffiths and Goodhew reported an average CO_2 storage of 316 tCO_2Eq. [76]. The exceptionally high MAETP levels recorded for both WSA–Br. and WSS-Min.w. scenarios were found to be related to the production of fired clay bricks contributing to at least 75% of MAETP. In particular, the production of 1 kg of bricks produces the emission of 10.6 mg hydrogen fluoride (HF) alongside a range of other chemicals of a high MAETP factor (4.07–5.38E07 kg 1,4-DCB-Eq per kg) [77].

4.4. Hot spots on GHG emissions

The results discussed in sections 4.1–4.3 show that emissions of GHG was by far the most affected impact category. In this section, LCA results

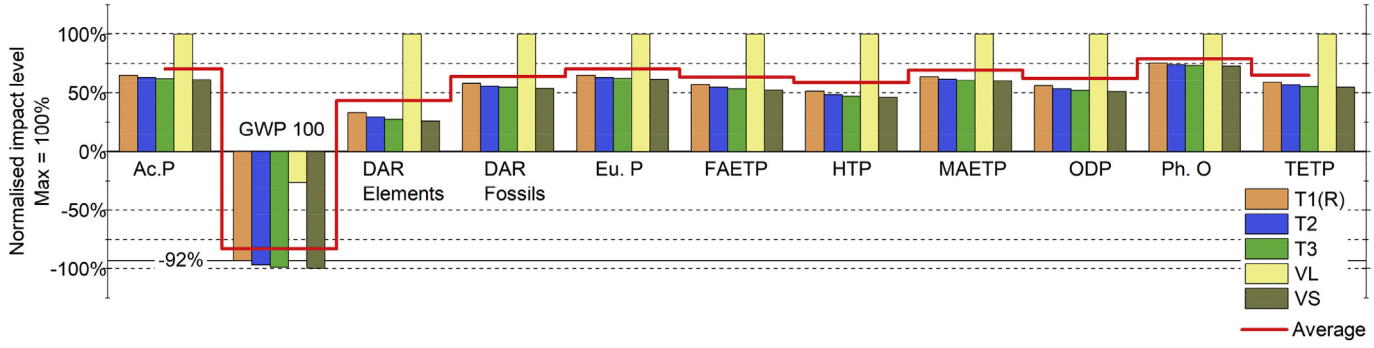

Fig. 12. Effect of transportation distances of binders on environmental impacts for the production of 1 m^3 of miscanthus concrete blocks. Results are normalized to maximum values across the impact categories.

Table 7
Impact categories levels for base scenario: the timber-framed wall filled with miscanthus concrete (WSA–Ti), miscanthus concrete replacing the insulation in a typical cavity wall (WSA–Br. scenario) and standard solid wall insulated with mineral wool (WSS-Min.w scenario).

Impact category	Abbreviations	Units	WSA-Br	WSA-Ti	WSS-Min.w
Acidification potential - average Europe	Ac.P	kg SO_2 eq.	4.72E-01	2.98E-01	3.97E-01
Climate change - GWP100	GWP 100	kg CO_2 eq.	31.16	−97.32	112.91
Depletion of abiotic resources - elements, ultimate reserves	DAR-Elements	kg Sb eq.	1.85E-04	1.01E-04	1.81E-04
Depletion of abiotic resources - fossil fuels	DAR-Fossils	MJ	1.46E+03	9.82E+02	1.05E+03
Eutrophication - generic	Eu.P	kg PO_4--- eq.	1.08E-01	7.39E-02	9.18E-02
Freshwater aquatic ecotoxicity - FAETP inf	FAETP	kg 1,4-DCB eq.	1.45E+01	1.21E+01	1.23E+01
Human toxicity - HTP inf	HTP	kg 1,4-DCB eq.	4.34E+01	2.70E+01	3.67E+01
Marine aquatic ecotoxicity - MAETP inf	MAETP	kg 1,4-DCB eq.	1.48E+05	2.64E+04	1.44E+05
Ozone layer depletion - ODP steady state	ODP	kg CFC-11 eq.	1.35E-05	1.01E-05	8.33E-06
Photochemical oxidation - high Nox	Ph.O	kg C_2H_4 eq.	3.39E-02	2.54E-02	2.41E-02
Terrestrial ecotoxicity - TETP inf	TETP	kg 1,4-DCB eq.	3.71E-01	2.97E-01	2.79E-01

were discussed for the production of 1 m^3 of miscanthus blocks and miscanthus wall assemblies to highlight elements of potential improvement. The results presented in Fig. 8 summarise the key steps involved in the production of miscanthus concrete blocks and their respective cumulative environmental impacts. It was shown that the production of miscanthus blocks remained by far the most critical step for most impact categories contributing for at least ~80% to all impact categories except for DAR-elements (65%). The overall net GHG emissions associated with the production of miscanthus concrete blocks were found to be ~−134.74 $kgCO_2eq/m^3$. The production of miscanthus blocks remains the process that contributes the most to GHG emissions with ~74.7% of positive emissions attributable to the production of binders (226.5 $kgCO_2eq/m^3$). The absorption of CO_2 achieved values ~−438.1 kg CO_2eq/m^3 of which 63.0% and 37.0% are attributable to miscanthus biogenic absorption and lime binder carbonation, respectively. The sensitivity analysis revealed that the reduction of binder to aggregate ratio leads to 32.9% and 72.7% decrease of GHG emissions, respectively for 2.0 to 1.5 and 3.0 to 1.5 binder to aggregate ratios reductions. On the other hand, the incorporation 10 wt% mineral additions (GGBS, OPC, FA) reduced the GHG emissions for less than 11.0%.

Wall assemblies incorporating miscanthus concrete (timber-framed and brick-cladded) performed better than the typical mineral wool insulated solid wall. Timber-framed wall benefits from both low energy processing of wood and its supplementary biogenic CO_2 capture. Timber-framed wall scenario (WSA–Ti) recorded carbon dioxide storage ~97.3 kg CO_2eq/m^2 with timber contribution of −9% and miscanthus shives biogenic CO_2 absorption of −35.8%. The brick cladded wall scenario (WSA–Br.) exhibited net GHG emissions ~31.16 kg CO_2eq/m^2, of which ~28.9% and 42% of positive emissions were attributed to the production of clay bricks and lime binder, respectively, for a total of 162.6 $kgCO_2eq/m^2$. The total recorded carbon dioxide sequestration (negative emissions) was −131.4 $kgCO_2eq/m^2$ of which ~63% and 37% were attributed to miscanthus biogenic CO_2 absorption and binder carbonation, respectively. The overall GHG emissions recorded for the standard mineral wool insulated wall scenario (WSS-Min.w) were ~113 $kgCO_2eq/m^2$. Fig. 14 shows the absolute percentage contribution from major processes to the GWP100 levels of all wall scenarios.

A comparative analysis of the obtained results with existing studies is difficult due to fundamental differences among models in terms of wall structure, functional unit definition and objectives of studies. Nevertheless, the actual results for timber-framed miscanthus wall can be compared to the UK study on hemp concrete walls carried out by Ip and Miller [24] and to the French studies of Boutin et al. [25] and Pretot et al. [78]. Ip and Miller reported a net GHG balance of −36 kg CO_2eq/m^2 for a 300 mm non-rendered, non-cladded wall while this study reports a net GHG balance of ~−97.4 kg CO_2eq/m^2 for a timber-framed wall. Though, this relatively high value is not directly attributable to miscanthus concrete blocks alone, but rather to the whole system and wall structure that include other significant contributions. Direct carbon dioxide capture attributable to miscanthus concrete blocks amounts to 69.5 $kgCO_2eq./m^2$ without considering the wood frame CO_2 capture of −27.9 kg CO_2eq. The French study of Boutin et al. [25] reported GHG emissions values of −35.53 kg CO_2eq/m^2. The fundamental differences in these studies lie in the low energy farming of miscanthus, its local availability that cuts down transportation-related impacts and high aggregate content of the investigated mixes that maximize biogenic CO_2 capture. For instance, in the study of Boutin et al., the energy associated with the production of hemp shiv is 2.1 MJ/kg while miscanthus shives production recorded an energy demand of 0.4 MJ/kg. In addition, miscanthus blocks in the present study contain 157 kg/m^3 of bio-aggregates while the hemp shives content of the walls in Boutin et al. is 95.38 kg/m^3 and 100 kg/m^3 in the study of Ip and Miller.

4.5. Limitations and assumptions

Life cycle analysis studies require the definition of scope and boundaries that impose assumptions in parameters of scenarios and hence, limitations in the interpretation of results. Major assumptions that

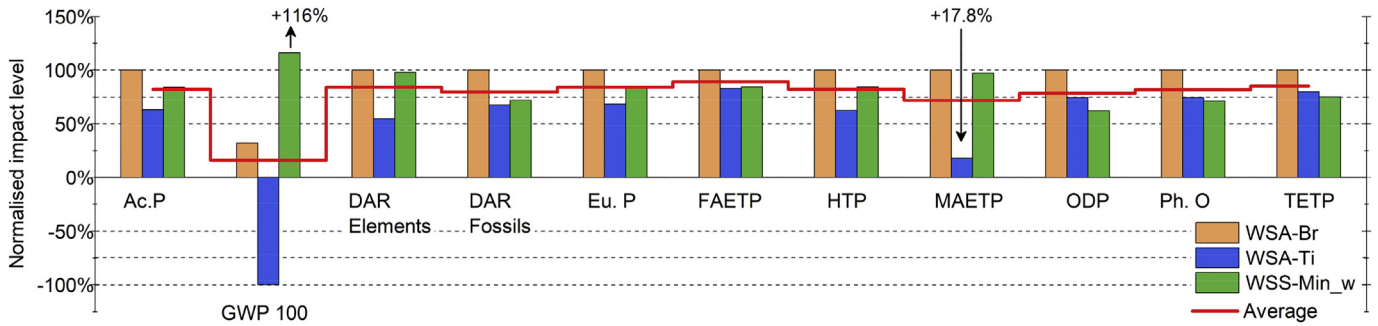

Fig. 13. Environmental impacts of blocks of miscanthus-lime wall assemblies and standard solid mineral wool insulated wall.

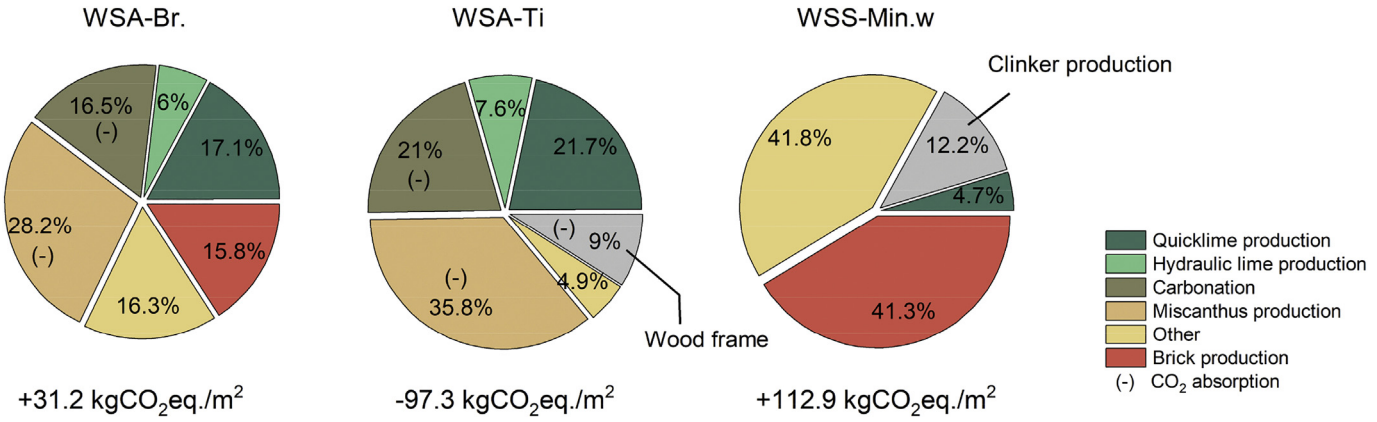

Fig. 14. Analysis of GHG emissions from wall assembly scenarios. The individual contribution of major processes to GWP100 at 1% cut-off.

were considered in this study were detailed in section 3.2. In light of this, the results should be interpreted with care and limited to analysed scenarios. At the wall assembly's analysis level, a large number of data entries obtained from generic databases make a profound analysis of results tedious as numerous background processes contribute largely to some impact categories. However, base cases of initial stages of miscanthus concrete block production provide sound and referenceable results with impacts traceable to individual processes and steps in the life cycle model. Some of the limitations of this study include the lack of sustainability thresholds for the reported levels of impact categories. On the other hand, inconsistencies across studies in terms of methods, functional units and systems boundaries make a transversal comparative analysis difficult. The use of pallets in transportation of products was interesting to consider in the model. However, it was not considered in the LCA model. The benefits associated with the growth of wood, its recycling and waste treatment could overshadow direct impacts from miscanthus concrete. The energy consumption associated with the storage of rhizomes at low temperatures was not considered in the LCA model. The end-of-life of bio-based building materials presents potential applications in recycling apart from standard landfilling. Crushed, they can be applied as lightweight aggregates orspread on agricultural soils to increase the pH [41]. Sierra-Pérez et al. have recently made assumptions and analysed cradle to gate, cradle to grave and cradle to cradle scenarios on a bio-based material [79]. Considering the lack of data for specific after-life applications and allied uncertainties [42], the analysis in the present paper was limited to a cradle-to-grave scenario for miscanthus concrete being transported and disposed in a local landfill. The same approach was adopted in literature for hemp-based bio-composites in wall structures [25,41,42].

5. Conclusion

Bio-based building materials present a viable potential as insulating materials. The recent growing awareness of sustainability in the construction sector, in large part due to the actual environmental concerns, has revitalized research interests on sustainable materials. Even though hemp-lime has emerged and remains widely used in buildings envelopes, miscanthus concrete has not been studied to any meaningful level compared to that of hemp concrete. In this study, an attempt was made to assess potential environmental impacts of incorporating miscanthus shives in lightweight blocks and the impact of miscanthus blocks on the overall life cycle of wall assemblies.

The reported results show that GHG emissions are the most affected environmental impact category through the variation of studied parameters across different scenarios. In fact, miscanthus blocks sequestrate GHG emissions that offset the binder production emissions to enable a storage of – 134.7 $kgCO_2eq/m^3$. The environmental implications of the system to a regional level could be significant. The association of miscanthus blocks with bricks cladding however lead to low emissions ~31.2 $kg\ CO_2eq/m^2$ while timber framing enhances the wall carbon storage levels ~−97.1 $kg\ CO_2eq/m^2$. The former could be potentially beneficial in retrofitting the existing brick walls and the latter in new-build houses.

The analysis of contributions from various factors show that binder content levels are the most influential factors for most of the environmental impact categories and for GWP100 in particular. Interestingly, the binder composition has a relatively little effect on GHG emissions. This infers even more flexibility in designing blends with mineral additions in the 10% range to improve the mechanical and durability performance of composites without significantly impacting their environmental performance. Although most of the overall GHG emissions are sequestered and stored with the incorporation of miscanthus concrete in wall assemblies, the environmental impacts associated with the farming of the crop remain to be considered and carefully accounted for. For instance, the use of miscanthus in timber framed wall and brick cladded walls (WSA-Ti and WSA–Br.) increased the ODP potential by 12.8% and 38%, respectively, compared to standard mineral wool insulated wall. However, the latter could be significantly reduced through the adoption of more environmentally friendly agricultural management practices. The lack of specific site data and the use of generic data from databases can have a significant impact on the accuracy of results. The use of site-specific data for local and regionally sourced materials can overcome these limitations and allow the application of results to the whole building life cycle assessment. Future work will focus on whole building model including operational energy and cost analysis. This will allow a scaling-up at national level considering the type and age of actual housing stock and identifying buildings that need retrofitting to conform to actual thermal performance requirements taking into account the potential carbon storage.

Credit author statement

Fabrice Ntimugura: Conceptualization, Methodology, Software, Data curation, Visualization, Investigation, Writing- Original draft preparation **Raffaele Vinai:** Conceptualization, Methodology, Validation, Writing - Review & Editing, Supervision, Project administration, Funding acquisition. **Anna B. Harper:** Conceptualization, Writing - Review & Editing, Supervision. **Pete Walker**: Conceptualization, Writing - Review & Editing, Supervision.

Acknowledgement and funding

This article is part of the ongoing research at the University of Exeter, College of Engineering Mathematics and Physical Sciences. This

research project is supported by a NERC GW4+ Doctoral Training Partnership studentship from the Natural Environment Research Council (NERC) and the National Productivity Investment Fund (NPIF) [NE/R011621/1]. The authors are thankful for the support and additional funding from CASE partners, Miscanthus Nursery Limited and Agrikinetics Limited. ABH acknowledges funding from EPSRC Fellowship EP/N030141/1 and NERC project NE/P019951/1. The assistance of Mike Cooper, David Stone and Ljwebber Richard with data collection at Lower Marsh Farm, is gratefully ackowledged.

Declaration of Competing Interest

The authors declare that they have no known competing financial interests or personal relationships that could have appeared to influence the work reported in this paper.

References

[1] D. Johnston, R. Lowe, M. Bell, An exploration of the technical feasibility of achieving CO2 emission reductions in excess of 60% within the UK housing stock by the year 2050, Energy Policy vol. 33 (13) (Sep. 2005) 1643–1659, https://doi.org/10.1016/j.enpol.2004.02.003.

[2] Vincent Nozahic, "Vers une nouvelle démarche de conception des bétons de végétaux lignocellulosiques basée sur la compréhension et l'amélioration de l'interface liant / végétal application à des granulats de chenevotte et de tige de tournesol associés à un liant ponce / chaux," Ph.D, Thesis, Université Clermont-Ferrand (2012) 2.

[3] M. Chabannes, E. Garcia-Diaz, L. Clerc, J.-C. Bénézet, F. Becquart, Lime Hemp and Rice Husk-Based Concretes for Building Envelopes, Springer International Publishing AG, Cham, Switzerland, 2017.

[4] Bio-aggregates based building materials:State-of-the-art report of the RILEM technical committee 236-BBM, in: S. Amziane, F. Collet (Eds.),Springer Netherlands, 2017.

[5] M.P. Sáez-Pérez, M. Brümmer, J.A. Durán-Suárez, A review of the factors affecting the properties and performance of hemp aggregate concretes, J. Build. Eng. 31 (Sep. 2020) 101323, https://doi.org/10.1016/j.jobe.2020.101323.

[6] "Dwelling stock estimates in England: 2019," *GOV.UK*. https://www.gov.uk/government/statistics/dwelling-stock-estimates-in-england-2019 (accessed Oct. 30, 2020).

[7] UK-housing-Fit-for-the-future-CCC-2019.pdf, , Accessed: Nov. 13, 2020. [Online]. Available https://www.theccc.org.uk/wp-content/uploads/2019/02/UK-housing-Fit-for-the-future-CCC-2019.pdf.

[8] I. Asadi, P. Shafigh, Z.F.B. Abu Hassan, N.B. Mahyuddin, Thermal conductivity of concrete – a review, J. Build. Eng. 20 (Nov. 2018) 81–93, https://doi.org/10.1016/j.jobe.2018.07.002.

[9] N. Pargana, M.D. Pinheiro, J.D. Silvestre, J. de Brito, Comparative environmental life cycle assessment of thermal insulation materials of buildings, Energy Build. vol. 82 (Oct. 2014) 466–481, https://doi.org/10.1016/j.enbuild.2014.05.057.

[10] R. Dylewski, J. Adamczyk, "12 - Life Cycle Assessment (LCA) of Building Thermal Insulation Materials," in *Eco-efficient Construction and Building Materials*, F. Pacheco-Torgal, L. F. Cabeza, J. Labrincha, and a, Eds. Woodhead Publishing, de Magalhães, 2014 267–286.

[11] G.A. Blengini, T. Di Carlo, The changing role of life cycle phases, subsystems and materials in the LCA of low energy buildings, Energy Build. 42 (6) (Jun. 2010) 869–880, https://doi.org/10.1016/j.enbuild.2009.12.009.

[12] F. Asdrubali, F. D'Alessandro, and S. Schiavoni, "a review of unconventional sustainable building insulation materials," *Sustain*, Mater. Technol. 4 (Jul. 2015) 1–17, https://doi.org/10.1016/j.susmat.2015.05.002.

[13] H. Binici, O. Aksogan, C. Demirhan, Mechanical, thermal and acoustical characterizations of an insulation composite made of bio-based materials, Sustain. Cities Soc. 20 (Jan. 2016) 17–26, https://doi.org/10.1016/j.scs.2015.09.004.

[14] M. Lawrence, Y. Jiang, Porosity, pore size distribution, micro-structure, in: S. Amziane, F. Collet (Eds.), Bio-Aggregates Based Building Materials:State-of-the-Art Report of the RILEM Technical Committee 236-BBM, Springer Netherlands, Dordrecht 2017, pp. 39–71.

[15] D. Peñaloza, M. Erlandsson, A. Falk, Exploring the climate impact effects of increased use of bio-based materials in buildings, Constr. Build. Mater. 125 (Oct. 2016) 219–226, https://doi.org/10.1016/j.conbuildmat.2016.08.041.

[16] C.R. Iddon, S.K. Firth, Embodied and operational energy for new-build housing: a case study of construction methods in the UK, Energy Build. 67 (Dec. 2013) 479–488, https://doi.org/10.1016/j.enbuild.2013.08.041.

[17] A. Azzouz, M. Borchers, J. Moreira, A. Mavrogianni, Life cycle assessment of energy conservation measures during early stage office building design: a case study in London, UK, Energy Build. 139 (Mar. 2017) 547–568, https://doi.org/10.1016/j.enbuild.2016.12.089.

[18] A. Estokova, S. Vilcekova, M. Porhincak, Analyzing embodied energy, global warming and acidification potentials of materials in residential buildings, Procedia Eng. 180 (Jan. 2017) 1675–1683, https://doi.org/10.1016/j.proeng.2017.04.330.

[19] M.J. González, J. García Navarro, Assessment of the decrease of CO2 emissions in the construction field through the selection of materials: practical case study of three houses of low environmental impact, Build. Environ. 41 (7) (Jul. 2006) 902–909, https://doi.org/10.1016/j.buildenv.2005.04.006.

[20] David Pickles, Energy efficiency and historic buildings. Insulating solid walls. Historic England, 2016, [Online]. Available https://historicengland.org.uk/images-books/publications/eehb-insulating-solid-walls/heag081-solid-walls/.

[21] M.L. Santarelli, F. Sbardella, M. Zuena, J. Tirillò, F. Sarasini, Basalt fiber reinforced natural hydraulic lime mortars: a potential bio-based material for restoration, Mater. Des. 63 (Nov. 2014) 398–406, https://doi.org/10.1016/j.matdes.2014.06.041.

[22] P. Pierquet, J.L. Bowyer, P.H. Huelman, Thermal performance and embodied energy of cold climate wall systems, For. Prod. J. 48 (6) (Jun. 1998) 53–60.

[23] R.M. Cuéllar-Franca, A. Azapagic, Environmental impacts of the UK residential sector: life cycle assessment of houses, Build. Environ. 54 (Aug. 2012) 86–99, https://doi.org/10.1016/j.buildenv.2012.02.005.

[24] K. Ip, A. Miller, Life cycle greenhouse gas emissions of hemp–lime wall constructions in the UK, Resour. Conserv. Recycl. 69 (Dec. 2012) 1–9, https://doi.org/10.1016/j.resconrec.2012.09.001.

[25] M.P. Boutin, C. Flamin, S. Quinton, G. Gosse, Etude des caractéristiques environnementales du chanvre par l'analyse de son cycle de vie, Ministère L'agriculture Pêche MAP 4 (2006) B1.

[26] A. Arrigoni, R. Pelosato, P. Melià, G. Ruggieri, S. Sabbadini, G. Dotelli, Life cycle assessment of natural building materials: the role of carbonation, mixture components and transport in the environmental impacts of hempcrete blocks, J. Clean. Prod. 149 (Apr. 2017) 1051–1061, https://doi.org/10.1016/j.jclepro.2017.02.161.

[27] J.H. Arehart, W.S. Nelson, W.V. Srubar, On the theoretical carbon storage and carbon sequestration potential of hempcrete, J. Clean. Prod. 266 (Sep. 2020) 121846, https://doi.org/10.1016/j.jclepro.2020.121846.

[28] F. Ntimugura, R. Vinai, A. Harper, P. Walker, Mechanical, thermal, hygroscopic and acoustic properties of bio-aggregates – lime and alkali - activated insulating composite materials: a review of current status and prospects for miscanthus as an innovative resource in the south west of England, Sustain. Mater. Technol. 26 (Dec. 2020), e00211. https://doi.org/10.1016/j.susmat.2020.e00211.

[29] Land use: Policies for a Net Zero UK, Committee on Climate Change, https://www.theccc.org.uk/publication/land-use-policies-for-a-net-zero-uk/ Jan. 2020, Accessed date: 18 June 2020.

[30] C. Emmerling, R. Pude, Introducing Miscanthus to the greening measures of the EU common agricultural policy, GCB Bioenergy 9 (2) (2017) 274–279, https://doi.org/10.1111/gcbb.12409.

[31] N. Ben Fradj, S. Rozakis, M. Borzęcka, M. Matyka, Miscanthus in the European bioeconomy: a network analysis, Ind. Crop. Prod. 148 (Jun. 2020) 112281, https://doi.org/10.1016/j.indcrop.2020.112281.

[32] R. Pude, C.H. Treseler, R. Trettin, G. Noga, Suitability of Miscanthus genotypes for lightweight concrete, Bodenkultur 56 (1/4) (2005) 61–69.

[33] L. Courard, V. Parmentier, Carbonated miscanthus mineralized aggregates for reducing environmental impact of lightweight concrete blocks, Sustain. Build. 2 (2017) 3, https://doi.org/10.1051/sbuild/2017004.

[34] Y. Chen, Q.L. Yu, H.J.H. Brouwers, Acoustic performance and microstructural analysis of bio-based lightweight concrete containing miscanthus, Constr. Build. Mater. 157 (Dec. 2017) 839–851, https://doi.org/10.1016/j.conbuildmat.2017.09.161.

[35] P.P. Dias, D. Waldmann, Optimisation of the mechanical properties of Miscanthus lightweight concrete, Constr. Build. Mater. 258 (Oct. 2020) 119643, https://doi.org/10.1016/j.conbuildmat.2020.119643.

[36] O. Ortiz, F. Castells, G. Sonnemann, Sustainability in the construction industry: a review of recent developments based on LCA, Constr. Build. Mater. 23 (1) (Jan. 2009) 28–39, https://doi.org/10.1016/j.conbuildmat.2007.11.012.

[37] I. Lewandowski, A. Heinz, Delayed harvest of miscanthus—influences on biomass quantity and quality and environmental impacts of energy production, Eur. J. Agron. 19 (1) (Feb. 2003) 45–63, https://doi.org/10.1016/S1161-0301(02)00018-7.

[38] M. Krzyżaniak, M.J. Stolarski, K. Warmiński, Life cycle assessment of giant miscanthus: production on marginal soil with various fertilisation treatments, Energies vol. 13 (8) (Jan. 2020) https://doi.org/10.3390/en13081931Art. no. 8.

[39] Z.M. Harris, S. Milner, G. Taylor, Chapter 5 - Biogenic Carbon—Capture and Sequestration, in: P. Thornley, P. Adams (Eds.), Greenhouse Gas Balances of Bioenergy Systems, Academic Press 2018, pp. 55–76.

[40] J.P. McCalmont, et al., Environmental costs and benefits of growing Miscanthus for bioenergy in the UK, Glob. Change Biol. Bioenergy vol. 9 (3) (Mar. 2017) 489–507, https://doi.org/10.1111/gcbb.12294.

[41] K. Ip, A. Miller, Life cycle greenhouse gas emissions of hemp–lime wall constructions in the UK, Resour. Conserv. Recycl. 69 (Dec. 2012) 1–9, https://doi.org/10.1016/j.resconrec.2012.09.001.

[42] S. Pretot, F. Collet, C. Garnier, Life cycle assessment of a hemp concrete wall: impact of thickness and coating, Build. Environ. 72 (Feb. 2014) 223–231, https://doi.org/10.1016/j.buildenv.2013.11.010.

[43] B. Berge, The Ecology of Building Materials, Routledge, 2009.

[44] Conservation of fuel and power: Approved Document L, GOV.UK, https://www.gov.uk/government/publications/conservation-of-fuel-and-power-approved-document-l (accessed Oct. 06, 2020).

[45] E. Latif, R. Bevan, T. Woolley, Thermal Insulation Materials for Building Applications, ICE Publishing, 2019.

[46] "Local Authority Building Control | LABC | Building control" https://www.labc.co.uk/ (accessed Oct. 08, 2020).

[47] V. Cérézo, Propriétés mécaniques, thermiques et acoustiques d'un matériau à base de particules végétales:approche expérimentale et modélisation théorique, PhD Thesis, Lyon, INSA, 2005.

[48] T.T. Nguyen, Contribution à l'étude de la formulation et du procédé de fabrication d'éléments de construction en béton de chanvre, phdthesis, Université de Bretagne Sud, 2010.

[49] F. Collet, S. Pretot, Thermal conductivity of hemp concretes: variation with formulation, density and water content, Constr. Build. Mater. 65 (Aug. 2014) 612–619, https://doi.org/10.1016/j.conbuildmat.2014.05.039.

[50] A. Andrianandraina, T.S. Ventura, B. Kiessé, R. Idir Cazacliu, H.M.G. van der Werf, Sensitivity analysis of environmental process Modeling in a life cycle context: a case study of hemp crop production, J. Ind. Ecol. 19 (6) (2015) 978–993, https://doi.org/10.1111/jiec.12228.

[51] M.F. Kocher, B.J. Smith, R.M. Hoy, J.C. Woldstad, S.K. Pitla, Fuel consumption models for tractor test reports, Trans. ASABE 60 (3) (2017) 693–701, https://doi.org/10.13031/trans.12121.

[52] D. Lovarelli, J. Bacenetti, Exhaust gases emissions from agricultural tractors: state of the art and future perspectives for machinery operators, Biosyst. Eng. 186 (Oct. 2019) 204–213, https://doi.org/10.1016/j.biosystemseng.2019.07.011.

[53] P. Smith, Soil carbon sequestration and biochar as negative emission technologies, Glob. Change Biol. 22 (3) (2016) 1315–1324, https://doi.org/10.1111/gcb.13178.

[54] T. Nakajima, T. Yamada, K.G. Anzoua, R. Kokubo, K. Noborio, Carbon sequestration and yield performances of Miscanthus × giganteus and Miscanthus sinensis, Carbon Manag. 9 (4) (Jul. 2018) 415–423, https://doi.org/10.1080/17583004.2018.1518106.

[55] "SimaPro LCA Software UK," *sim-org*. https://www.simapro.co.uk (accessed Feb. 25, 2020).

[56] GaBi for Universities, http://www.gabi-software.com/uk-ireland/software/gabi-universities/ (accessed Feb. 25, 2020).

[57] LCA Software for Life Cycle Assessment - Umberto LCA+, ifu Hamburg GmbH, Feb. 20, 2020. https://www.ifu.com/en/umberto/lca-software/ (accessed Feb. 25, 2020).

[58] "Quantis | Tool Development," *Quantis*. https://quantis-intl.com/tools/software/tool-development/ (accessed Feb. 25, 2020).

[59] "openLCA modeling suite | openLCA.org." /openlca/ (accessed Feb. 25, 2020).

[60] A. Ciroth, ICT for environment in life cycle applications openLCA — a new open source software for life cycle assessment, Int. J. Life Cycle Assess. 12 (4) (Jun. 2007) 209, https://doi.org/10.1065/lca2007.06.337.

[61] LINGO and optimization modeling, https://www.lindo.com/index.php/products/lingo-and-optimization-modeling (accessed Oct. 08, 2020).

[62] I.P. Stanimirovic, M.L. Zlatanovic, M.D. Petkovic, On the linear weighted sum method for multi-objective optimization, 2011 15.

[63] A. Azapagic, R. Clift, Life cycle assessment and multiobjective optimisation, J. Clean. Prod. 7 (2) (Mar. 1999) 135–143, https://doi.org/10.1016/S0959-6526(98)00051-1.

[64] B. Berge, C. Butters, F. Henley, Chapter 6 - Minerals, in: B. Berge, C. Butters, F. Henley (Eds.), The Ecology of Building Materials (Second Edition), Architectural Press, Oxford 2009, pp. 71–105.

[65] D. Higgins, Briefing: GGBS and sustainability, Proc. Inst. Civ. Eng. - Constr. Mater. 160 (3) (Aug. 2007) 99–101, https://doi.org/10.1680/coma.2007.160.3.99.

[66] P.W. Gerbens-Leenes, A.Y. Hoekstra, R. Bosman, The blue and grey water footprint of construction materials: steel, cement and glass, Water Resour. Ind. 19 (Jun. 2018) 1–12, https://doi.org/10.1016/j.wri.2017.11.002.

[67] V. Prado, B.A. Wender, T.P. Seager, Interpretation of comparative LCAs: external normalization and a method of mutual differences, Int. J. Life Cycle Assess. 22 (12) (Dec. 2017) 2018–2029, https://doi.org/10.1007/s11367-017-1281-3.

[68] V. Castellani, L. Benini, S. Sala, R. Pant, A distance-to-target weighting method for Europe 2020, Int. J. Life Cycle Assess. 21 (8) (Aug. 2016) 1159–1169, https://doi.org/10.1007/s11367-016-1079-8.

[69] Z. Luca, S. Erwan, S. Erwin, C.G. Jorge, C. Valentina, S. Serenella, *Guide for interpreting life cycle assessment result*. LU: publications, Office EUR 28266 EN (2016) 60, https://doi.org/10.2788/171315.

[70] European Commission and Joint Research Centre, ILCD handbook, General Guide for Life Cycle Assessment:Detailed Guidance, Publications Office of the European Union, Luxembourg, 2010.

[71] H.L. Tuomisto, I.D. Hodge, P. Riordan, D.W. Macdonald, Exploring a safe operating approach to weighting in life cycle impact assessment – a case study of organic, conventional and integrated farming systems, J. Clean. Prod. 37 (Dec. 2012) 147–153, https://doi.org/10.1016/j.jclepro.2012.06.025.

[72] A. Bjørn, M.Z. Hauschild, Introducing carrying capacity-based normalisation in LCA: framework and development of references at midpoint level, Int. J. Life Cycle Assess. 20 (7) (Jul. 2015) 1005–1018, https://doi.org/10.1007/s11367-015-0899-2.

[73] S. Sala, A.K. Cerutti, R. Pant, Development of a weighting approach for the Environmental Footprint, Publications Office of the European Union, Luxembourg, 2018https://doi.org/10.2760/945290 ISBN 978-92-79- 68042-7, EUR 28562.

[74] G. Huppes, L. van Oers, U. Pretato, D.W. Pennington, Weighting environmental effects: analytic survey with operational evaluation methods and a meta-method, Int. J. Life Cycle Assess. 17 (7) (Aug. 2012) 876–891, https://doi.org/10.1007/s11367-012-0415-x.

[75] A.S. Smith, P. Bingel, A. Bown, 11 - sustainability of masonry in construction, Sustainability of Construction Materials, Second editionEd. Woodhead Publishing, J. M. Khatib 2016, pp. 245–282.

[76] R. Griffiths, S. Goodhew, Sustainability of solid brick walls with retrofitted external hemp-lime insulation, Struct. Surv. 30 (4) (Jan. 2012) 312–332, https://doi.org/10.1108/02630801211256661.

[77] R. Hischier, et al., Implementation of life cycle impact assessment methods, p. 176, 2010.

[78] S. Pretot, F. Collet, C. Garnier, Life cycle assessment of a hemp concrete wall: impact of thickness and coating, Build. Environ. 72 (Feb. 2014) 223–231, https://doi.org/10.1016/j.buildenv.2013.11.010.

[79] J. Sierra-Pérez, J. Boschmonart-Rives, A.C. Dias, X. Gabarrell, Environmental implications of the use of agglomerated cork as thermal insulation in buildings, J. Clean. Prod. 126 (Jul. 2016) 97–107, https://doi.org/10.1016/j.jclepro.2016.02.146.